
# Exciton dynamics in molecular solids from line shape analysis: An assessment of the extent of line shape distortion resulting from use of real crystals

G. C. Morris and M. G. Sceats

Citation: The Journal of Chemical Physics **60**, 375 (1974); doi: 10.1063/1.1681052

View online: http://dx.doi.org/10.1063/1.1681052

View Table of Contents: http://scitation.aip.org/content/aip/journal/jcp/60/2?ver=pdfcov

Published by the AIP Publishing



# Exciton dynamics in molecular solids from line shape analysis: An assessment of the extent of line shape distortion resulting from use of real crystals

**G. C. Morris and M. G. Sceats**

*Department of Chemistry, University of Queensland, St. Lucia, Qld. 4067, Australia*
(Received 3 October 1972)

For crystal absorption systems, the line profile of the frequency dependence of the dielectric permittivity $\epsilon(\omega)$ contains information about the exciton dynamics that may be studied by the autocorrelation function generated by the Fourier transformation of $\epsilon(\omega)$ into the time domain. However, $\epsilon(\omega)$ obtained through transforming normal incidence reflectance data $R(\omega)$ of a real crystal when the photon–crystal eigenmodes are strongly coupled may be considerably distorted from $\epsilon(\omega)$ of a perfect infinite crystal. In this paper, we consider the ways by which such distortions may arise and, by using a model for $\epsilon(\omega)$ that might reasonably correspond to the 4000 Å $b$-polarized 0–0 absorption system at low temperatures of crystalline anthracene probed on the (001) face, we illustrate the dependence of the extent of distortions on the line profile of $\epsilon(\omega)$ upon the following number of factors, viz., (i) spatial dispersion of the exciton bands; (ii) use of an oblique angle of incidence as an approximation to normal incidence in determining $R(\omega)$; (iii) thickness of the crystal slab used to determine $R(\omega)$; (iv) extent of roughness on the crystal surface; (v) mole fraction of defects in the crystal; and (vi) mole fraction of impurities in the crystal. The treatment allows definition of the condition [real $\epsilon(\omega) < 0$] under which various quasiparticles (longitudinal excitons, surface excitons, excitons bound to impurities) may be excited in a particular crystal system. The methods employed in this paper are of general applicability to strongly absorbing crystal systems and will be of use in understanding exciton dynamics in such systems. The data provide a firm foundation for interpreting reflectance data of a strongly absorbing crystal system, and thus we are able to discuss existing spectral data for anthracene crystals, especially narrow structure observed in low temperature reflection spectra, as well as suggest areas for both theoretical and experimental work.

## I. INTRODUCTION

The primary mechanism of electronic energy transfer in a molecular solid is governed by the exciton (or polariton)–phonon interaction. Yet despite its importance, little information is available on the dynamical properties of molecular excitons especially in the situation when the photon–crystal eigenmodes are strongly coupled (i.e., when the oscillator strength per unit cell is moderately large along given polarization and propagation directions). For the case of weak coupling between the photon and crystal eigenmodes, there are methods of probing certain aspects of exciton dynamics.[1] For the strong coupling case, we have developed an approach to this problem through a determination of the frequency dependence of the dielectric permittivity $\epsilon(\mathbf{k}, \omega)$ obtained from transformation of normal incidence reflectance data $R(\omega)$.[2] The line profiles of $\epsilon_r(\mathbf{k}, \omega)$ and $\epsilon_i(\mathbf{k}, \omega)$, the real and imaginary parts, respectively, of $\epsilon(\mathbf{k}, \omega)$, contain information on exciton (or polariton in this case) dynamics. Two methods are useful for relating these data to meaningful parameters describing the dynamics. First, the autocorrelation function $C(t)$ of the scattering processes which is closely related to the double time retarded Green function of the system may be generated by Fourier transformation of $\epsilon(\mathbf{k}, \omega)$ into the time domain. This approach gives physical insight into the scattering processes because of correspondence of classical and quantum mechanical processes in the time domain.[3] Second, a comparison of $\epsilon(\mathbf{k}, \omega)$ at various temperatures with functions derived from models of exciton–phonon scattering theory should indicate the adequacy of a particular model.[3,4]

These methods of data analysis are useful when $\epsilon(\mathbf{k}, \omega)$ generated experimentally is undistorted from the correct $\epsilon(\mathbf{k}, \omega)$ describing exciton–phonon (or polariton–phonon) scattering in infinite perfect crystals. In general, the correct $\epsilon(\mathbf{k}, \omega)$ may be distorted by (i) experimental imprecisions in measuring $R(\omega)$ and (ii) the use of a finite, imperfect crystal instead of a semi-infinite perfect crystal to obtain raw data $R(\omega)$

An absolute error of 0.02 in $R(\omega)$ $(0 \leq R \leq 1)$ may produce an error of 30% in $\epsilon_i(\mathbf{k}, \omega)$.[5] This error is larger than the errors induced by the transformation methods[5] giving $\epsilon(\mathbf{k}, \omega)$ from $R(\omega)$.

For a finite perfect crystal, excitation of surface and longitudinal modes, effects due to the finite radiative lifetime of the exciton, effects from interference of the modes with odd and even parity about the center of the crystal, and effects from use of an oblique angle of incidence as an approximation to normal incidence light will distort $R(\omega)$ of a semi-infinite perfect crystal. For imperfect crystals the existence of irregularities on the surface and impurities, defects or in general inhomogeneities in the bulk, also perturb $R(\omega)$.

It is possible to refine the experimental design to an extent where $R(\omega)$ for a perfect crystal is obtained with a precision of $\pm 0.001$ which in the crystal system discussed in this paper leads to errors in $\epsilon(\mathbf{k}, \omega)$ of the same magnitude as arises from use of transformation methods, viz., 4%.[5] But to what extent does the use in experiments of a finite imperfect crystal rather than an infinite perfect crystal invalidate an approach to understanding the exciton's dynamics through interpretation

  

of the line shape of $\epsilon(\mathbf{k}, \omega)$? We seek an answer to this important question in this paper.

There are a number of intense electronic transitions in molecular crystals for which, following our approach, reflectance spectroscopy will be needed to probe the static properties of the exciton and provide data from which the dynamic properties may be deduced. To provide a sound basis for our arguments, we seek an answer to the question raised in the last paragraph by considering the 4000 Å $b$-polarized 0–0 crystal transition of anthracene, for which pertinent experimental data at low temperatures have been obtained by Morris *et al.*[2] This is not to be seen as a limitation of the approach of the present paper because the methods employed are not specific to the absorption system considered. But it is necessary to assess numerous effects upon the absorption profile by using a model of $\epsilon(\omega)$ that might reasonably correspond to some crystal absorption system. In view of the wealth of experimental and theoretical data existing on the anthracene lowest singlet–singlet crystal transition,[6] this system provides a convenient test situation. In anticipation of the results of this paper, it would appear that to obtain meaningful information on the dynamics of the exciton in any strongly absorbing perfect crystal by interpretation of $\epsilon(\mathbf{k}, \omega)$ measured on a real crystal, it will be necessary to apply the methods of this paper to ensure that the measured $\epsilon(\mathbf{k}, \omega)$ approximates that of the perfect crystal. Of course, the band profile of $\epsilon(\mathbf{k}, \omega)$ distorted in a real crystal from that of a perfect crystal may be used to probe exciton dynamics in a real crystal and so understand more clearly the role which impurities, defects, and inhomogeneities play in determining such dynamics.

In essence, the procedure followed is to obtain the line profile of $\epsilon(\omega)$ under various conditions for a perfect semi-infinite crystal and for ranges of finite crystals and of imperfect semi-infinite crystals. This line profile is compared with that of a model of a perfect infinite anthracene crystal. From these data it is possible to gauge, for negligible distortion of $\epsilon(\omega)$ of the model, (i) the lower bounds of $m^*$, the exciton effective mass in a specific propagation direction; (ii) the upper bounds of $\phi$, the angle of incidence of the photon beam on the crystal when probing $R(\omega)$; (iii) the lower bounds of $d$, the thickness of the crystal used to determine $R(\omega)$; (iv) the upper bound on $NV$, the average surface roughness, assuming that the distorted regions are much less in all dimensions than the wavelength of light; (v) the upper bound on $\sigma$, the rms roughness, which mainly governs incoherent photon scattering from the surface; (vi) the upper bound of $\eta$, the percentage by volume of defects in the crystal, under the same assumption as (iv); (vii) the mole fraction of impurities in the crystal in both the amalgamation and persistence limits when the impurities form either shallow or deep lying traps, but neglecting certain resonance effects.

The treatment allows definition of the conditions under which various quasiparticles may be excited in a particular crystal system. These quasiparticles (longitudinal excitons, surface excitons, excitons bound by impurities, etc.) cause the majority distortion in $\epsilon(\mathbf{k}, \omega)$. The data obtained provide a firm foundation for interpreting experimental reflectances and thus we are able to discuss existing data, suggest a number of useful experiments, and indicate areas where further theoretical work is needed.

## II. MODEL EMPLOYED

The model for $\epsilon(\mathbf{k}, \omega)$ is that for the 4000 Å $b$-polarized 0–0 transition of a perfect and infinite anthracene crystal at 7 °K. Assume that the frequency dependence of the dielectric permittivity $\epsilon(\omega)$ of a perfect infinite anthracene crystal is the Lorentzian profile generated by Helmholz–Kettler oscillators

$$\epsilon(\omega) = \epsilon_r(\omega) + i\epsilon_i(\omega) = \epsilon_0 + 4\pi\rho\omega_0^2/(\omega^2 - \omega_0^2 - i\gamma\omega) , \qquad (1)$$

where $\epsilon_0$ is the background dielectric permittivity, $\rho$ is the oscillator strength, $\omega_0$ the resonant frequency [where $\omega\epsilon_i(\omega)$ is maximum], and $\gamma$ the damping parameter. Note that the model assumes that the crystal is composed of a set of noninteracting oscillators thus leading to an independence of $\epsilon$ on $\mathbf{k}$. The function chosen corresponds to an exponential falloff of the correlation function $C(t)$ describing exciton dynamics and should describe the optical band profile in the case of weak exciton–phonon scattering when dispersion of the exciton band and the $\mathbf{k}$, $\omega$ variation of the self energy are neglected. Temperature effects are simulated by variation of $\gamma$, i.e., all nonradiative processes such as intensity stealing are considered temperature independent. Appropriate values of the parameters determining $\epsilon(\omega)$ could be[2] $\epsilon_0 = 6.4$, $\rho = 0.01$, $\omega_0 = 25127$ cm$^{-1}$, and $\gamma = 75$ cm$^{-1}$. The anthracene crystal is anisotropic with two molecules per unit cell, but because of the simplified nature of the model used, the crystal is assumed isotropic with one isotropic molecule per unit cell. Hence, we will not obtain explicit information on how the use of finite imperfect crystals affects experimental data on properties such as Davydov splitting, which are dependent upon multiple molecules per unit cell, although certain implicit data are obtained. It would be a useful application of the work of this paper to use a model which should simulate $R(\omega)$ obtained with light polarized along crystal directions other than the $b$-crystal direction as well as allowing for multiple molecules per unit cell.

## III. DISTORTION OF THE MODEL CAUSED BY VARIOUS EFFECTS

### A. Effects from use of semi-infinite perfect crystals

In this section, we consider how $\epsilon(\omega)$ of the model might be distorted by effects which would occur even in semi-infinite perfect crystals and evaluate the extent of such distortions from three causes: (i) spatial dispersion, (ii) damping of longitudinal modes, (iii) experimental use of non-normal angles of incidence as an approximation to a perfect normal incidence experiment to obtain $R(\omega)$.

Recent calculations on cubic[7] and monoclinic (anthracene)[8] crystals have shown that the dipole interactions between planes of molecules normal to $\mathbf{k}$ (the exciton wave vector) fall off so rapidly that only near neighbor

interactions between planes need be used to evaluate the effects on $\epsilon(\omega)$ of spatial dispersion.[9] Since only adjacent planes need be considered, two polariton modes would exist in the semi-infinite crystal,[7] and one boundary condition, in addition to the usual two Maxwell conditions, is needed to solve for the crystal eigenmodes. This extra boundary condition is that a linear combination of the polarization ($\mathbf{P}$) and its derivative ($\partial\mathbf{P}/\partial x$) vanishes at the surface.[10] If the exciton is the stable eigenmode of the system then $\mathbf{P}=0$ is the relevant boundary condition.[11] But the condition can be met only near and not at the surface for Wannier excitons,[12] and the effect of this is that structure is induced in $R(\omega)$ near the frequency of the $\mathbf{k}=0$ polariton, i.e., near $\omega_L$. If the polariton is the stable eigenmode, this structure occurs regardless of the boundary conditions[13] and indicates the general breakdown of the fields within the crystal so that no normal modes exist. As indicated elsewhere,[2] for this anthracene crystal transition, the polariton is the stable eigenmode since the radiative width of the polariton is less than the stopping bandwidth ($\omega_L - \omega_0$). Hence some structure from this effect may appear in $R(\omega)$.

To determine the extent of effects from noninfinite effective mass of the exciton (effects of spatial dispersion) and from excitation of longitudinal modes, we use a dispersion relationship with a pole

$$(\omega_p + \hbar k^2/2m_p^*)e^{i\theta_p}$$

and a zero

$$(\omega_z + \hbar k^2/2m_z^*)e^{i\theta_z}$$

in the complex frequency plane, so that

$$\epsilon(\mathbf{k},\omega) = \epsilon_0 \frac{\omega_z^2 + (\hbar/m_z^*)k^2\omega_z - \omega^2 - i\Gamma_z\omega}{\omega_p^2 + (\hbar/m_p^*)k^2\omega_p - \omega^2 - i\Gamma_p\omega}, \tag{2}$$

where $m_z^*$, $m_p^*$ are the exciton effective masses and $\Gamma_p(\mathbf{k},\omega)$, $\Gamma_z(\mathbf{k},\omega)$ are the damping parameters for the pole and zero, respectively. This relationship is an extension of that used by Hopfield and Thomas[12] in that the pole and zero are given different effective masses and damping parameters. When $m_z^*$ and $m_p^* \to \infty$, this relationship is the general dispersion relationship used by Berreman and Unterwald[14] to fit Restrahlen data and by us to fit anthracene crystal reflectance data.[2]

### 1. Effects of spatial dispersion

Equation (2) was solved for the refractive index $n$ ($=k\omega$) to give two complex solutions $\hat{n}_1(\omega)$ and $\hat{n}_2(\omega)$. Using the additional boundary condition $\mathbf{P}=0$, the effective refractive index $\hat{n}_e(\omega)$

$$\hat{n}_e(\omega) = [\hat{n}_1(\omega)\hat{n}_2(\omega) + \epsilon_0]/[\hat{n}_1(\omega) + \hat{n}_2(\omega)], \tag{3}$$

effective dielectric permittivity $\epsilon_e(\omega) = \hat{n}_e(\omega)^2$, and normal incidence reflectance $R(\omega)$

$$R(\omega) = |[\hat{n}_e(\omega) - 1]/[\hat{n}_e(\omega) + 1]|^2 \tag{4}$$

are each generated.

An estimate of the extent of the effects of spatial dispersion may be determined by calculating the dependence of the shape of $R(\omega)$, $\hat{n}_e(\omega)$, and $\epsilon_e(\omega)$ on the value of $m_p^*$. To do this using the simple model of Sec. II, let $\Gamma_p = \Gamma_z = \gamma$ and $\omega_z = \omega_p\,[1 + (4\pi\rho/\epsilon_0)]^{1/2}$. The data are collected in Table I and displayed in Fig. 1. Note that the use of the "exciton" boundary condition does not generate structure at $\omega_z$. Further, as expected, the spectrum was calculated to be insensitive to the value of $m_z^*$ ($\geq 10\ m_e$). Calculations of the exciton band structure of anthracene[15] accounting for dipolar dispersions indicate that the dispersion for $\mathbf{k}$ normal to the ($ab$) monoclinic face is very small ($m^* > 1000\ m_e$). Hence from Table I spatial dispersion will have little effect upon the crystal spectrum parallel (or perpendicular) to $b$ unless through the dispersion of $\Gamma_z$ or $\Gamma_p$. Further, it is worth noting that the values calculated for $\hat{n}_2(\omega)$ [$=n_2(\omega) + i\kappa_2(\omega)$] show that $n_2(\omega)$ and $\kappa_2(\omega)$ are very large, while $\hat{n}_1(\omega)$ has values close to that generated by the Lorentzian function when $m_p^*$ and $m_z^* \to \infty$. In Table II the values of $n_2(\omega)$ and $\kappa_2(\omega)$ are summarized for different values of $m_p^*$, where $m_z^* = m_p^*$. The large values of $n_2(\omega)$ and $\kappa_2(\omega)$ indicate that the second mode is "mechanical" or excitonlike [slow, $n_2(\omega)$ large] and localized near the surface [$\kappa_2(\omega)$ large].[7]

TABLE I. Effects of spatial dispersion on the maximum values of optical parameters of a perfect semi-infinite anthracene crystal.

| Parameter | Value for perfect, Infinite crystal (Lorentzian model) | Value for perfect crystal with various exciton effective mass in units of rest mass of electron (percentage change from infinite crystal case in brackets.) $10^0$ | $10^1$ | $10^2$ | $10^3$ | $10^4$ | $10^5$ |
|---|---|---|---|---|---|---|---|
| $R\left(=\left\|\frac{n-1}{n+1}\right\|^2\right)$ | 0.71160 at | 0.66720 | 0.69722 | 0.70701 | 0.71014 | 0.71113 | 0.71145 |
| | 25190 $cm^{-1}$ | (6.24) | (2.02) | (0.65) | (0.21) | (0.07) | (0.02) |
| $\epsilon_i(=2n\kappa)$ | 42.0724 at | 33.679 | 39.124 | 41.105 | 41.763 | 41.974 | 42.021 |
| | 25126 $cm^{-1}$ | (9.95) | (7.01) | (2.30) | (0.74) | (0.23) | (0.12) |
| $\kappa$ | 4.7782 at | 4.2093 | 4.5833 | 4.7151 | 4.7581 | 4.7718 | 4.7762 |
| | 25146 $cm^{-1}$ | (11.91) | (4.08) | (1.32) | (0.42) | (0.13) | (0.04) |
| $n$ | 5.6934 at | 5.1865 | 5.5170 | 5.6365 | 5.6753 | 5.6877 | 5.6916 |
| | 25102 $cm^{-1}$ | (8.90) | (3.10) | (1.00) | (0.32) | (0.10) | (0.03) |

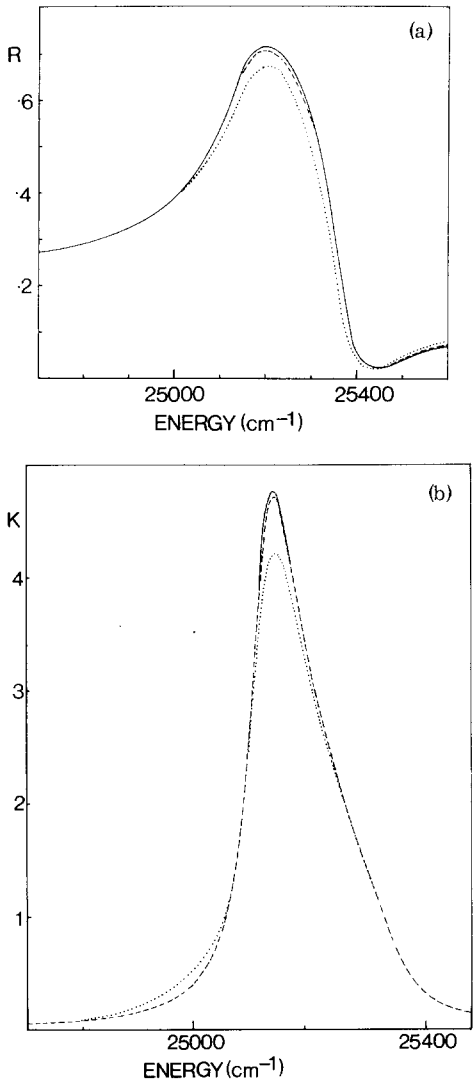


FIG. 1. The effect of finite values of exciton effective mass ($m_p^*$) on the reflectance $R(\omega)$ 1(a) and absorption index $\kappa(\omega)$ (b) of a perfect semi-infinite anthracene crystal. Solid line, $m_p^* = \infty$; dotted line $m_p^* = m_e$ (rest mass of an electron); dashed line $m_p^* = 100\ m_e$.

### 2. *Effects from damping of the longitudinal modes*

To calculate the effects due to spatial dispersion, it was assumed for simplicity that $\Gamma_p(\mathbf{k}, \omega) = \Gamma_z(\mathbf{k}, \omega)$, i.e., the lifetimes of the pole and zero were the same. Relaxing that restriction, we now evaluate the effects on the optical parameters in the limit $m_p^*$ and $m_z^* \to \infty$. The method followed is to set initially $\Gamma_p$ $(= 2\omega_p \sin\theta_p)$ as $(\omega_z/\omega_p)\ \Gamma_z = 75\ \text{cm}^{-1}$ using the parameters characterizing the model of Sec. II. In that case, $\omega_z = \omega_0[1 + (4\pi\rho/\epsilon_0)]^{1/2} = 25\,372\ \text{cm}^{-1}$. Then, $\Gamma_z$ $(= 2\omega_z \sin\theta_z)$ is allowed to assume various values. Some results are shown in Table III and Fig. 2. We note the following points:

(i) Increasing $\Gamma_z$ causes positive asymmetry in $\epsilon_i(\omega)$. The maximum values of $\epsilon_r$, $\epsilon_i$ and $n$ are all increased while those of $R$ and $\kappa$ decrease.

(ii) For $\Gamma_z > \Gamma_p$, the maximum value of $\epsilon_i$ (energy absorbed per unit time per unit volume) increases, while the maximum value of $\kappa$ (decrease in energy flux per unit distance along $\mathbf{k}$) decreases.

TABLE II. Dependence of the refractive index and absorption index of the "mechanical" mode upon the exciton effective mass $(m^*_p)$.

| Exciton effective mass (units of rest mass of electron) | Refractive index $n_2$ at 25 126 $\text{cm}^{-1}$ | Absorption index $\kappa_2$ at 25 126 $\text{cm}^{-1}$ |
|---|---|---|
| $10^0$ | 38.4 | 39.4 |
| $10^1$ | 122 | 125 |
| $10^2$ | 386 | 397 |
| $10^3$ | 1224 | 1257 |
| $10^4$ | 3870 | 3975 |
| $10^5$ | 12238 | 12569 |

(iii) For $\Gamma_z < \Gamma_p$, the maximum values of both $\epsilon_i$ and $\kappa$ decrease, indicating that $\epsilon_i$ is a minimum for the symmetric case.

(iv) A large maximum refractive index is indicative of strong positive asymmetry in $\epsilon_i(\omega)$ and the position of the maximum of $R(\omega)$ is a very sensitive function of the asymmetry.

(v) The resonance frequency $\omega_0$ and the maximum val-

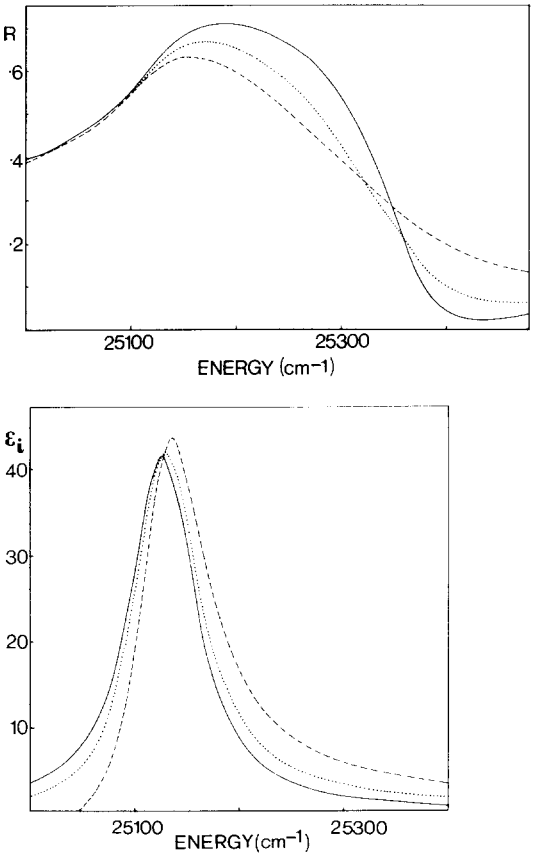


FIG. 2. The effect of the damping parameters upon the reflectance $R(\omega)$ 2(a) and the imaginary part of the dielectric permittivity $\epsilon_i(\omega)$ (b) of a perfect semi-infinite anthracene crystal. The background dielectric permittivity is 6.4; the frequency of the pole $(\omega_p)$ is 25127 $\text{cm}^{-1}$ and that of the zero $(\omega_z)$ is 25 372 $\text{cm}^{-1}$. $\text{Sin}\theta_p = 0.0015$ (damping parameter $\Gamma_p = 2\omega_p \sin\theta_p$) for each graph. Solid line, $\sin\theta_z = 0.0015$ (damping parameter $\Gamma_p = 2\omega_z \sin\theta_z$); dotted line, $\sin\theta_z = 0.003$; dashed line, $\sin\theta_z = 0.006$.

ue of $\epsilon_i(\omega)$ become separated with asymmetry. Large positive asymmetry may move the maximum position of $\epsilon_i(\omega)$ some 20 $cm^{-1}$ higher than $\omega_0$.[16]

(vi) When $\Gamma_z \neq \Gamma_p$, the induced asymmetry produces negative $\epsilon_i(\omega)$ values which are noncausal. In fact, Eq. (2) gives solutions which are causal over the whole frequency range for only a very limited set of $\Gamma_z$. This may be indicated as follows. If $\omega_z^2 = \omega_0^2(1+x)$, then $\epsilon_i(\omega)$ is negative when

$$\omega^2 > \omega_0^2\{1 - [\Gamma_p/(\Gamma_z - \Gamma_p)]x\} = \omega_a^2, \quad \Gamma_p > \Gamma_z \tag{5}$$

$$\omega^2 < \omega_0^2\{1 + [\Gamma_p/(\Gamma_p - \Gamma_z)]x\} = \omega_a^2, \quad \Gamma_z > \Gamma_p, \tag{6}$$

Values of $\omega_a$ have been listed in Table III also. A causal solution over all $\omega$ will occur for $\Gamma_z$ in the very small range $\Gamma_p \leq \Gamma_z \leq \Gamma_p(1+x)$, although values of $\Gamma_z$ outside this range may adequately represent spectra when effects of other transitions approximated by $\epsilon_0$ result in behavior such that $\epsilon(\omega)$ is causal. As $|\Gamma_p - \Gamma_z|$ becomes large, the noncausal regions of $\omega$ come close to the experimental regions of interest. Obviously values of $\Gamma_z$ should be chosen so that $\omega_a$ does not come close to $\omega_0$ or $\omega_z$. To do so when asymmetry is marked would require frequency dependent damping parameters $\Gamma_p(\omega)$ and $\Gamma_z(\omega)$ to describe the spectrum. This will almost certainly be the case for the crystal system considered.[17]

### *3. Effects from use of non-normal angles of incidence to obtain normal incidence reflectance data*

In this section we evaluate the effects which arise when, as an experimental approximation to normal incidence light, the photon beam is incident on the crystal at some angle to the normal other than 0°. When large cones of convergence of the light beam are used, such non-normal incidence effects are also important in distorting $R(\omega)$.

Consider a beam of parallel rays which is incident at an angle $\phi$ to the normal upon the (001) face of an anthracene crystal with the $b$-crystal axis in the plane of incidence. Assuming a uniaxial crystal of isotropic molecules[18] for $p$-polarized light, define an effective dielectric permittivity $\epsilon_e(\omega)$

$$\epsilon_e(\omega) = [\epsilon_c(\omega)\epsilon_b(\omega)\cos^2\phi]/[\epsilon_c(\omega) - \sin^2\phi] = [n_e(\omega)]^2. \tag{7}$$

The reflectance $R_p(\omega)$ is given by

$$R_p(\omega) = \left| [\epsilon_c(\omega)^{1/2} - 1]/[\epsilon_e(\omega)^{1/2} + 1] \right|^2. \tag{8}$$

In Eqs. 7 and 8, $\epsilon_b(\omega)$ is the dielectric permittivity for light polarized along the $b$-crystal axis and normal to the (001) plane and $\epsilon_c(\omega)$ is the dielectric permittivity for light polarized along the $c$-crystal axis and normal to the (010) plane. As a simple but suitable approximation, let $\epsilon_b(\omega)$ and $\epsilon_c(\omega)$ each be represented by a Lorentzian line dielectric function model generated by Helmholz–Kettler oscillators. For $\epsilon_b(\omega)$, the parameters are those of the model of Sec. II. For $\epsilon_c(\omega)$ $(\equiv \epsilon_a(\omega))$, when **k** is normal to the (001) crystal face and the light is polarized parallel to the $a$-crystal axis, suitable values are $\epsilon_0 = 4.0$, $\omega_0 = 25\,300$ $cm^{-1}$, $\rho = 0.0015$, and $\gamma = 50$ $cm^{-1}$. Using various values of $\phi$, the values of $\epsilon_e(\omega)$, $n_e(\omega)$, and $R_p(\omega)$ were calculated. Some results are shown in Table IV,

TABLE III. Effect upon the maxima of the optical parameters and the frequency at which these occur caused by the finite lifetime of the longitudinal modes. The lifetime of the pole ($\tau_p = 1/2\omega_p \sin\theta_p$) is constant with $\sin\theta_p = 0.0015$ ($\equiv 75.38$ $cm^{-1}$).

| Optical parameter | $\Gamma_z = 1/\tau_z$ (in units of $2\omega_z$) | | | | | | | | | | |
|---|---|---|---|---|---|---|---|---|---|---|---|
| | 0.00001 | 0.0001 | 0.0005 | 0.0010 | 0.0015 | 0.002 | 0.003 | 0.005 | 0.0075 | 0.009 |
| $R$ | 0.8849 | 0.8028 | 0.7626 | 0.7319 | 0.7094 | 0.6918 | 0.6662 | 0.6386 | 0.6287 | 0.6296 |
| $\omega$ $cm^{-1}$ | 25370 | 25271 | 25224 | 25203 | 25190 | 25183 | 25171 | 25159 | 25152 | 25149 |
| $\epsilon_r$ | 24.40 | 24.56 | 25.32 | 26.31 | 27.36 | 28.46 | 30.80 | 36.22 | 43.96 | 49.03 |
| $\omega$ $cm^{-1}$ | 25084 | 25084 | 25086 | 25088 | 25090 | 25093 | 25098 | 25103 | 25106 | 25108 |
| $\epsilon_i$ | 42.50 | 42.02 | 41.89 | 41.83 | 41.78 | 41.83 | 42.05 | 43.12 | 45.58 | 47.32 |
| $\omega$ $cm^{-1}$ | 25124 | 25124 | 25126 | 25126 | 25127 | 25128 | 25130 | 25134 | 25138 | 25140 |
| $n$ | 5.466 | 5.478 | 5.531 | 5.604 | 5.679 | 5.760 | 5.933 | 6.321 | 6.861 | 7.200 |
| $\omega$ $cm^{-1}$ | 25100 | 25100 | 25101 | 25102 | 25103 | 25104 | 25106 | 25110 | 25112 | 25114 |
| $\kappa$ | 5.000 | 4.984 | 4.914 | 4.832 | 4.756 | 4.685 | 4.561 | 4.380 | 4.262 | 4.236 |
| $\omega$ $cm^{-1}$ | 25144 | 25144 | 25144 | 25146 | 25146 | 25147 | 25148 | 25152 | 25156 | 25158 |
| $\omega_a$ $cm^{-1}$ | 25374 | 25390 | 25495 | 25870 | | 24404 | 24884 | 25023 | 25066 | 25078 |

where only the variations and errors at the maximum values of $R$, $\epsilon_i$, and $\kappa$ and minimum values of $\epsilon_r$ and $n$ are shown. The percentage errors in the optical parameters vary significantly with frequency so leading to distortion of the lines profile when non-normal angles of incidence are used. This is more clearly shown in Fig. 3. From Table IV and Fig. 3, we note the following points:

(i) For errors in $R$ of less than 0.1% at the peak, $\phi$ must be less than 6°. This error in $R(\omega)$ leads to only small errors in $\epsilon_i(\omega)$ and $\epsilon_r(\omega)$, but note that these calculations have been carried out under the assumption that $\omega_0$ is independent of $\mathbf{k}$. However as Philpott[15b] has shown the energy of $\lim_{\mathbf{k}\to 0}\omega(\mathbf{k})[\mathbf{k}\perp(001)]$ is about 650 $cm^{-1}$ below the energy of $\lim_{\mathbf{k}\to 0}\omega(\mathbf{k})[\mathbf{k}\perp(010)]$. Hence the $\mathbf{k}$ independence of $\omega_0$ is a crude approximation for this crystal system and the errors in Table IV are to be regarded as a lower limit.

(ii) The relative distortion in $\kappa(\omega)$ is less than the relative distortion in the other optical parameters.

(iii) As $\kappa$ increases with increasing $\phi$, $\epsilon_i$ $(=2n\kappa)$ decreases.

(iv) For large $\phi$, a small hump appears in $\epsilon_i(\omega)$ (see Fig. 3) near 25 300 $cm^{-1}$ corresponding to the transition expected when light is polarized perpendicular to the $b$ axis. No shift in the frequency of the maximum of $\epsilon_i$ or $R$ is observed in the spectrum because, in the calculations, the $\mathbf{k}$ dependence of the resonance frequency was not taken into account. However the measured resonance frequency is a strong function of the angle of incidence.

The above data lead us to suggest that oblique angle spectroscopy can probe $\mathbf{k}$ space around $\mathbf{k}=0$ to give exciton dispersion. The varying angle oblique incidence spectra will map aspects of the exciton band structure. Preliminary experimental results appear to confirm this

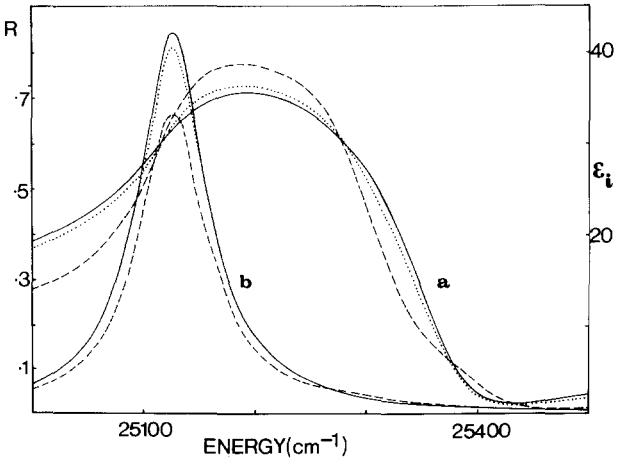


FIG. 3. The effect on $R(\omega)$ (a) and $\epsilon_i(\omega)$ 3(b) by use of non-normal incidence light as an approximation to normal incidence light, upon a perfect semi-infinite anthracene crystal. The data are calculated assuming the anthracene crystal is uniaxial, that the light is $P$ polarized and incident at an angle of $\phi$ on the (001) face with the $b$ axis in the plane of incidence. The values of the parameters used are given in the text. Solid line, $\phi=0$; dotted line, $\phi=20°$; dashed line, $\phi=45°$.

TABLE IV. Variations in the maximum values (for $R$, $\epsilon_i$, $\kappa$) or minimum value (for $\epsilon_r$, $n$) of the optical parameters and the frequency at which each occurs caused by use of various angles of incidence of the photon beam on a perfect semi-infinite anthracene crystal. Percentage variation in brackets.

| Optical parameter | Angle of incidence of the photon beam on crystal | | | | | | | | | | | |
|---|---|---|---|---|---|---|---|---|---|---|---|---|
| | 0° | 6° | 9° | 12° | 15° | 18° | 21° | 24° | 27° | 30° | 33° | 36° |
| $R$ at | 71.16 | 71.27 | 71.41 | 71.60 | 71.85 | 72.15 | 72.51 | 72.93 | 73.40 | 73.92 | 74.51 | 75.15 |
| 25 190 $cm^{-1}$ | | (0.15) | (0.35) | (0.62) | (0.97) | (1.4) | (1.9) | (2.5) | (3.1) | (3.9) | (4.7) | (5.6) |
| $\epsilon_r$ at | −14.45 | −14.55 | −14.67 | −14.84 | −15.06 | −15.32 | −15.63 | −15.99 | −16.38 | −16.81 | −17.28 | −17.78 |
| 25 160 $cm^{-1}$ | | (0.69) | (1.5) | (2.7) | (4.2) | (6.0) | (8.2) | (10.7) | (13.4) | (16.3) | (19.6) | (23.0) |
| $\epsilon_i$ at | 41.83 | 41.69 | 41.52 | 41.28 | 40.96 | 40.57 | 40.11 | 39.56 | 38.92 | 38.20 | 37.38 | 36.46 |
| 25 130 $cm^{-1}$ | | (0.34) | (0.74) | (1.3) | (2.1) | (3.0) | (4.1) | (5.4) | (6.9) | (8.7) | (10.6) | (12.8) |
| $n$ at | 0.5739 | 0.5773 | 0.5815 | 0.5874 | 0.5949 | 0.6039 | 0.6143 | 0.6261 | 0.6392 | 0.6534 | 0.6687 | 0.6850 |
| 25 320 $cm^{-1}$ | | (0.59) | (1.3) | (2.8) | (3.6) | (5.2) | (7.0) | (9.1) | (11.4) | (13.9) | (16.5) | (19.4) |
| $\kappa$ at | 4.760 | 4.765 | 4.771 | 4.779 | 4.790 | 4.804 | 4.819 | 4.836 | 4.856 | 4.877 | 4.900 | 4.925 |
| 25 150 $cm^{-1}$ | | (0.11) | (0.23) | (0.40) | (0.63) | (0.92) | (1.2) | (1.6) | (2.0) | (2.4) | (2.9) | (3.5) |

but further experiments are needed to determine fully the feasibility of the method. Of course, one could use a set of different crystal faces to achieve the same goal. The results of Clark and Philpott[19] using a few different crystal faces do show that the resonance frequency alters from one crystal face to another, as expected, but it may be easier to use oblique angle spectroscopy on a specific crystal face rather than a range of crystal faces which for molecular crystals are difficult to prepare.

Also, oblique angle spectroscopy is a possible method for probing properties of longitudinal modes in a molecular crystal. From Eq. (7), it is observed that a resonance will occur in $\epsilon_e(\omega)$ when $\epsilon_c(\omega) = \sin^2\phi$. In the frequency region where this occurs, $\epsilon_c(\omega)$ passes through zero from negative values. Considering $\epsilon_b(\omega)$ and $\epsilon_c(\omega)$ real, the behavior of $R_p(\omega)$ near this region varies as follows: it decreases to zero when $\epsilon_c(\omega) = -(\sin^2\phi)/[\epsilon_b(\omega)\cos^2\phi - 1]$ (note that this corresponds to the Brewster's condition for total transmission); it is unity from $\epsilon_c(\omega) = 0$ to $\sin^2\phi$ (at which $\epsilon_e(\omega)$ resonates); and it decreases as $\epsilon_c(\omega)$ becomes more positive. Hence, one would expect in an oblique angle reflection experiment to observe structure in $R_p$ which would be a narrow dip when $\partial\epsilon_c/\partial\omega$ is large. This structure would be centered around the frequency of the longitudinal mode ($\omega_L$) for the longitudinal optic modes propagate at a frequency $\omega_L$ such that $\epsilon = 0$ when damping is neglected (longitudinal waves have no electric displacement accompanying them).[20] When damping is included, one expects a longitudinal mode to occur when $\epsilon$ has a minimum absolute value. For a biaxial crystal such as anthracene, a number of longitudinal modes will exist and may propagate along specific directions, although Brewster's condition is probably met along many directions of the incident light beam in strong crystal absorptions. However, is structure [a dip in $R_p(\omega)$] observed in an oblique angle of incidence experiment near the expected frequency of a longitudinal mode to be taken as prima facie evidence for the excitation and frequency $\omega_L$ of a longitudinal mode? Such an interpretation is not without its problems, prominent among which is that a breakdown in the internal electric field normal to the crystal surface may be caused by other factors and structure in $R_p(\omega)$ will occur from these even in a normal incidence experiment.[12] In other words, a dip in $R(\omega)$ may occur near $\omega_L$ for reasons other than propagation of a longitudinal mode. However, oblique angle spectroscopy has been used to probe the value of $\omega_L$ in the infrared spectra of films,[20] crystals,[21] and of polycrystalline aggregates.[22]

In the light of the above discussion we can make some tentative explanations of features observed in the $b$-polarized low temperature reflectance spectrum of an anthracene crystal when a non-normal beam of incident photons is used.[23,24] Within and to higher energies of the main $b$-polarized absorption band, the broadest and most prominent of these narrow decreases in $R(\omega)$ occurs near 25 290 $cm^{-1}$. It is unstable in frequency and intensity, as well as varying with experimental arrangement and crystal thickness. It is most prominent when the $b$-crystal axis and the polarization vector lay in the plane of incidence ($P$ polarization). Possibly this marks a frequency region where $\epsilon$ is near zero so that the electric field normal to the surface is broken down within the crystal. It may be evidence for the position of a longitudinal mode. The frequencies of the longitudinal modes should be higher in energy than 25 290 $cm^{-1}$ in the infinite crystal.[15] Strains in the real crystal could shift the expected $\omega_L$ as this value is sensitive to changes of surface charge. Also for a crystal of finite size, calculations[15a] indicate that the longitudinal exciton band structure at small $\mathbf{k}$ values varies with crystal size so that a double peaked density of longitudinal states is expected, with one peak at $\omega_L$ of an infinite crystal and the other some several hundred wave numbers lower in energy. In a preliminary observation at 4 °K using 45° incidence light on the $b$ axis with the polarization vector in the plane of incidence, there is a reflectance dip near 25 480 $cm^{-1}$ which might mark the frequency $\omega_L$ in the infinite crystal. Only further work will decide.[25]

To illustrate how such a reflectance dip may be generated when $\phi = 45°$, in a sample calculation we generate $R_p(\omega)$ using a general dispersion analysis[2] rather than the Lorentzian line dielectric function model since the former and not the latter is a good fit of experimental data in the region of $\omega_L$. This is shown in Fig. 4. Note the dip in $R_p(\omega)$ becomes more pronounced as the background dielectric constant $\epsilon_0$ increases and the damping parameter $\gamma$ decreases. For this calculation, the damping parameter was considered to be frequency independent which is an unrealistic approximation in the vicinity of $\omega_L$. Perhaps a damping parameter proportional to $\mathbf{k}^2$ which would vanish at $\omega_L$ ($\mathbf{k} = 0$) for excitons of large effective mass as developed in a recent polariton–phonon scattering theory[26] would be useful in this regard. However, the elementary calculation used to produce Fig. 4 does show how reflectance dips may develop near $\omega_L$. Such structure is not unambiguous evidence of the

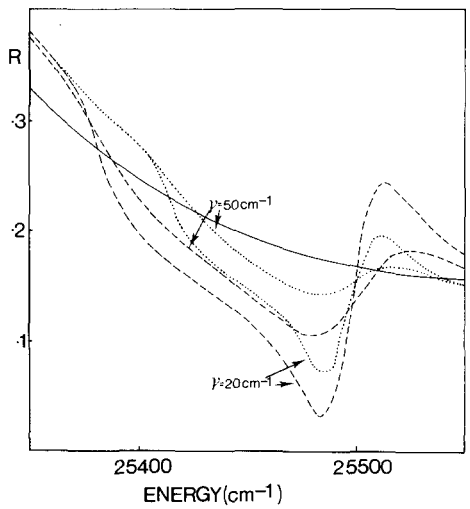


FIG. 4. Introduction of structure in $R(\omega)$ near the frequency of the longitudinal mode when light is incident on a perfect semi infinite anthracene crystal at an angle of 45°. Note how the structure becomes more pronounced with decreasing damping parameter $\gamma$ and increasing value of the background dielectric permittivity $\epsilon_0$ of the $ac$ crystal transition. Solid line, unperturbed $R(\omega)$ at normal incidence; dotted line, $\epsilon_0 = 3$; dashed line, $\epsilon_0 = 4$.

excitation and frequency of the longitudinal modes, however, as the condition for this occurrence may be fulfilled by other means. We would suggest that clearer evidence would be obtained by observing the angular dependence of the intensity of $R_p(\omega)$ in the region where $\omega_L$ is expected. To our knowledge, this has not been done for any crystal system in any spectral region, but in virtue of the importance of determining properties of the longitudinal modes by a means as simple as oblique angle reflection spectroscopy, it would be very useful.

### B. Effects from use of a finite perfect crystal

In this section, we consider the effects on $\epsilon(\omega)$ which might arise by use of a perfect crystal of finite thickness for measurement of $R(\omega)$ and hence $\epsilon(\omega)$. In an infinite crystal, the radiative lifetime of an exciton is infinite,[27] so that neglecting damping, Agranovich's theory[28] predicts a real refractive index which is infinite at the resonant frequency. Hence for absorption to occur, the polariton must scatter from a third body,[29] e.g., phonons. For a finite crystal, however, nonperiodic boundary conditions exist and with the exciton and photon no longer quantized in the same volume radiative damping can occur.[30] We now consider the minimum crystal size before this effect and the consequent distortion of $\epsilon(\omega)$ of the infinite crystal becomes important. Before achieving this it is necessary to consider the surface states which may be excited.

#### *1. Surface states excited in a finite perfect crystal neglecting retardation*

Considering near neighbor interactions and neglecting retardation of the electromagnetic fields, the normal modes of a crystal in which all the molecules experience the same short range interactions are of two types[31]: bulk (oscillatory spatial dependence with frequencies $\omega_0$ and $\omega_L$) and surface (exponential decay across the crystal). The bulk modes are standing waves within the crystal and are characterized by discrete values of the wave vector $\mathbf{k}$ normal to the slab. The two surface modes are characterized by their dependence on the component of the wave vector $k_x$ parallel to the slab and only exist for $P$ polarization. For a crystal of thickness $2a$, then if $k_x a \gg 1$, the surface modes are localized near the surface and have frequencies between $\omega_0$ and $\omega_L$; but, as $k_x a \to 0$, the modes become delocalized at $\omega_L$ and $\omega_0$ and no surface modes are excited by normal incidence light.

Even if the above surface modes which originate from the long range Coulomb forces do not exist in a crystal, transverse surface modes may arise from the change in the short range forces at $k_x a = 0$. These modes retain their surface character at $k_x a = 0$ and are localized—their amplitudes decay rapidly into the crystal within a lattice constant. Such modes have been discussed for phonons in ionic crystals.[32] For the molecular excitons of interest in this paper, surface excitations of this type occur when the change in energy of the surface molecules due to the alteration of the short range forces exceeds the electronic bandwidth due to dipole dispersion.[33] The electronic bandwidth, as measured by the stopping bandwidth, is about 200 $cm^{-1}$.[2] The environmental shift of an anthracene molecule in a crystal due to short range interactions has contributions from dispersion forces, first order effects from intermolecular interactions, dipole–dipole interactions to about 50 Å, higher multipoles, and exchange forces. The shift is dominated by the dispersion forces being approximately $-2700$ $cm^{-1}$ for a molecule within the crystal.[34] For a molecule within the surface layer, approximately 75% of the interactions may be active, giving a shift in the resonant frequency of the surface modes of approximately 700 $cm^{-1}$. Hence using the Sugakov[33] criterion, it is expected that surface modes would be excited.

#### *2. Surface states excited in a finite perfect crystal including retardation*

For a model in which the change in the short range interactions at the surface are neglected, the modes of the crystal may be separated into two types—radiative and nonradiative—when retardation is included.[35,36] If $\epsilon(\omega)$ for an infinite crystal is given by Eq. (1), the nonradiative modes exist for $k_x > \omega/c$, where $k_x = \mathbf{k}\sin\phi$ ($\phi$ is angle of incidence). Define

$$\alpha = (k_x^2 - \omega^2/c^2)^{1/2} , \tag{9}$$

$$\beta = [\epsilon(\omega)\omega^2/c^2 - k_x^2]^{1/2} . \tag{10}$$

Then the radiative modes are given by the solutions of

$$\epsilon(\omega) = \frac{i\beta}{\alpha}\,\frac{e^{-i\beta a} \pm e^{i\beta a}}{e^{-i\beta a} \mp e^{i\beta a}} \tag{11}$$

for $P$ polarization and

$$1 = \frac{i\beta}{\alpha}\,\frac{e^{-i\beta a} \pm e^{i\beta a}}{e^{-i\beta a} \mp e^{i\beta a}} \tag{12}$$

for $S$ polarization. Solutions exist when $k_x > \omega/c$ and $< \epsilon^{1/2}\omega/c$. These solutions decay exponentially ($e^{-\alpha|z|}$) outside the surface.

The radiative modes have progressive wave solutions outside the crystal and thus interact with light in a normal optical experiment. The nonradiative modes are exponentially damped outside the crystal and do not interact with light except in special circumstances. Thus surface roughness may induce the excitation of surface exciton modes by destroying the pure nonradiative character of the modes, as discussed later.

There has been no experimental evidence for these nonradiative modes in a molecular crystal, but our calculations show that they could be detected by means of light that is exponentially damped in space with a complex angle of incidence generated by a prism of appropriate refractive index placed a small distance from the crystal (frustrated total reflection).[37] Such experiments leading to a detection measurement of the dispersion of these surface modes are now in progress.

For the radiative modes, when light is incident on the crystal surface, momentum is conserved only in directions parallel to the surface. The excited polariton state then has a radiative width which is dependent on the angle of incidence and which will be very large at the Brewster angle (see Sec. III, A, 3). These radiative effects may cause distortion of the frequency dependence of the opti-

cal constants and this distortion will be a function of crystal thickness owing to the long range nature of the forces involved. To determine the thickness of an anthracene crystal where such effects become observable, we have calculated $R(\omega)$ for crystals of different thickness and with an angle of incidence of $\phi = 0$. For $\phi = 0°$, we may write $R(\omega)$ as

$$R(\omega) = \left| \frac{1 - (1/\hat{n}(\omega))^2}{1 + \left(\frac{1}{\hat{n}(\omega)}\right)^2 + 2\frac{1}{\hat{n}(\omega)} \left| \frac{1 + e^{4i\hat{n}(\omega)a\omega/c}}{1 - e^{4i\hat{n}(\omega)a\omega/c}} \right|} \right|^2$$

$$= \left| \frac{\hat{n}^2(\omega) - 1}{\hat{n}^2(\omega) + 1 + 2\hat{n}(\omega) \left| \frac{1 + e^{4i\hat{n}(\omega)a\omega/c}}{1 - e^{4i\hat{n}(\omega)a\omega/c}} \right|} \right|^2 . \quad (13)$$

Since $\hat{n}(\omega) = \hat{n}_r(\omega) + i\kappa(\omega)$, then, provided $\kappa(\omega) \neq 0$,

$$\frac{1 + e^{4i\hat{n}(\omega)a\omega/c}}{1 - e^{4i\hat{n}(\omega)a\omega/c}} \to 1$$

as the crystal thickness $2a \to \infty$. In this thickness limit, Eq. (13) will reduce to

$$R(\omega) = \left| \frac{\hat{n}(\omega) - 1}{\hat{n}(\omega) + 1} \right|^2 , \quad (14)$$

i.e., the Fresnel formula for normal incident light on a semi-infinite crystal. Hence, in the limit of infinite thickness, the effect of radiative damping is negligible at $\phi = 0$ provided that a finite damping due to third body interactions exists.

When $\phi \neq 0°$, the effect of radiative damping upon $R(\omega)$ in a semi-infinite crystal may be calculated as in Sec. III. A. 3 when account is taken of the anisotropic nature of the crystal.

In Fig. 5 graphs of $R(\omega)$ for different crystal thickness are shown calculated using values of parameters for the infinite crystal model. From Fig. 5 we make the following observations.

(i) For a crystal of thickness greater than 1 $\mu$, $R(\omega)$ is sensibly independent of thickness, i.e., effects of radiative broadening are negligible.

(ii) For a crystal of thickness near 0.1 $\mu$, distortions appear below $\omega_0$ and above $\omega_L$ from effects related to the spreading out of the transverse low and high energy modes.

(iii) For a crystal of thickness near 0.01 $\mu$, the effects of radiative damping are severe. The spectrum is shifted some 95 $cm^{-1}$ to lower energies by one of the high energy modes passing through the "blocking band" region to lower energies. It had been inferred previously, [6] that a transmission experiment on a thin crystal (~0.05 $\mu$) leads to an incorrect absorption band profile and incorrect absorption intensity mainly because of the nonpenetration of the absorption band. Our current data demonstrate clearly that absorption (and reflection) spectroscopy on a thin crystal will not produce reliable spectral data for a strongly absorbing crystal system when the effects from radiative damping are severe. It suggests that caution should be exercised when interpreting spectra from thin films.

It would seem that the use of anthracene crystals of thickness greater than 1 $\mu$ will give reflectance spectra with a shape determined by third body interactions provided the crystal is otherwise perfect.

### 3. *Interference effects*

Finally in this section we comment upon the possibility of distortions arising from interference effects even in crystals which are thick enough for $R(\omega)$ to be determined by third body interactions. In an optical experiment with light incident on one face of a crystal, modes which are mixtures of the solutions symmetric and antisymmetric about the crystal center may be excited and cause interference effects in $R(\omega)$, $T(\omega)$, and $A(\omega)$, where $T(\omega)$ is the transmission and $A(\omega)$ $[= 1 - T(\omega) - R(\omega)]$ is the absorption. The amplitude of the interference effect will be dependent on crystal thickness, angle of incidence and the damping parameter.

In Fig. 6, we show $R(\omega)$ and $\kappa(\omega)$ for normal incidence light on a crystal of 10 $\mu$ thickness with different damping parameters. The effect becomes negligible as the damping parameter increases and also as the crystal thickness increases. At small values of $\gamma$, however, the absorption exhibits interference effects associated with excitation of crystal eigenmodes and the amplitude of the interference is a measure of the damping processes ($\gamma$) at a given thickness. Little effect from this is likely to be observed within the absorption region for crystals thick enough for reflectance measurements determined by third body interactions, but is readily observed outside the absorption region.

## C. Effects from use of a real semi-infinite crystal

In previous sections, it has been shown that $\epsilon(\omega)$ of the model may be distorted even in a perfect crystal under conditions where the longitudinal modes are excited (i.e., oblique incidence) or a crystal of insufficient thickness is used to measure $R(\omega)$. If these effects are avoided by use of perfect normal incidence radiation on a crystal of sufficient thickness, what distortion of $\epsilon(\omega)$ will arise

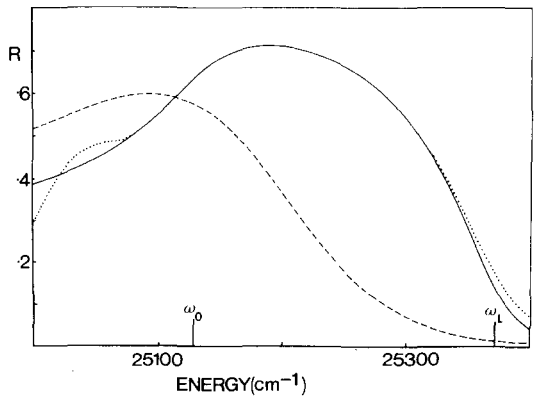


FIG. 5. The dependence of the normal incidence reflectance $R(\omega)$ on the thickness of an anthracene crystal. Calculations based on a model of $\epsilon(\omega)$ as described in the text with $\omega_0$ and $\omega_L$ the frequencies of the transverse and longitudinal modes respectively. Solid line, $1\mu = 10\mu = \infty$; dotted line, $0.1\mu$; dashed line, $0.01\mu$.

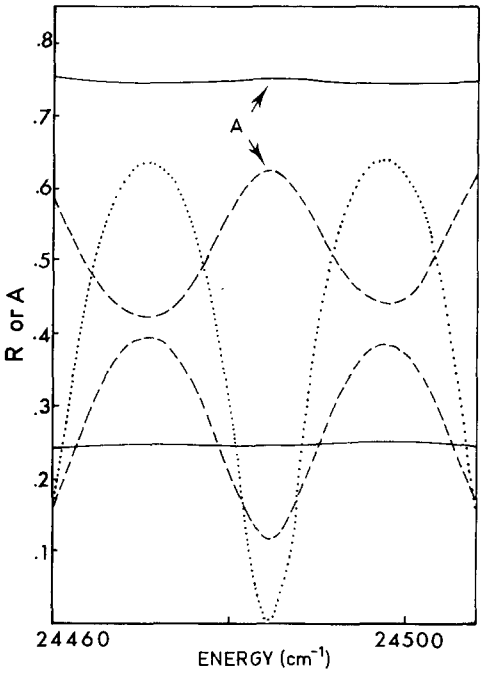


FIG. 6. The effect of the magnitude of the damping parameter ($\gamma$) upon the normal incidence reflectance $R(\omega)$ and the absorption $A(\omega)$ of a perfect anthracene crystal of 10 $\mu$ thickness. Dotted line, $\gamma = 0$ cm$^{-1}$; dashed line, $\gamma = 10.0$ cm$^{-1}$; solid line, $\gamma = 25.0$ cm$^{-1}$.

because the crystal is not perfect but has rough surfaces and edges as well as defects, impurities, voids or in general bulk inhomogeneities. In an earlier publication[2] some of these effects were considered. We now extend the area of that work and render it more quantitative.

### 1. Surface roughness

The surface of a real semi-infinite molecular crystal is expected to be rough. This may allow the excitation of roughness induced surface excitons. It will also cause a decrease in reflectivity via two mechanisms: incoherent scattering and coherent scattering.

Incoherent (diffuse) scattering arises from phase fluctuations, caused by different path lengths of different rays upon reflection from the crystal surface. The interference of the reflected waves is no longer completely constructive in one (specular) direction. The normal incidence specular reflection from a rough surface when incoherent scattering occurs may be expressed[38] as

$$R(\omega) = R_0(\omega)\, e^{-(4\pi\sigma/\lambda)^2} \qquad (15)$$

for a Gaussian distribution of irregularities where $\sigma$ is the rms roughness related to the rms height of the bumps. $R_0(\omega)$ is the reflectance from a perfectly smooth surface. The wavelength dependence of the distortion due to incoherent scattering from Eq. (15) is not marked. Since, as noted previously[2] the major problem preventing an accurate measure of $R(\omega)$ is the diffuse scattering some method of quantitatively determining the extent of its effect is desirable. Over a small frequency range, such as the resonance region, a correction for incoherent scattering is obtainable if $R_0(\omega)$ is known accurately at some nearby frequency and if Eq. (15) is adequate. Accurate measures of the refractive index at some frequency outside the absorption region obtained by other means provides a value of $R_0(\omega)$. From the measured $R(\omega)$ at the same frequency $\sigma$ may be calculated. We have determined $\sigma$ for a range of crystals by accurately measuring $R(\omega)$ at room temperature. A report of that work will be published later. For the purpose of this paper, we note that accurate measurement of $R(\omega)$ at 4200 Å on crystals of thickness such that the back surface reflection is negligible provide values of $\sigma \approx 100$ Å in solution grown aged crystals, but much lower values ($\approx 50$ Å) in sublimation flakes.

Of course any correction procedure using Eq. (15) assumes that the reflection spectrometer does not accept a significant amount of the incoherent scattered light. The reflectance $R(\omega)$ measured in a spectrometer when some of the incoherent scattering is detected may be expressed[39] by

$$R(\omega) = R_0(\omega)[e^{-(4\pi\sigma/\lambda)^2} + (2^5\pi^4/m^2)(\sigma/\lambda)^4(\Delta\theta)^2]\,, \qquad (16)$$

where $\Delta\theta$ is the acceptance angle of the spectrometer in steradians and $m$ is the rms slope of the surface profile. The amount of diffuse light collected $[(\equiv R_0(\omega)(2^5\pi^4/m^2) \times (\sigma/\lambda)^4(\Delta\theta)^2]$ in a specific reflectometer may be calculated using different values of $\sigma$ and $m$. A good approximation to the value of $\sigma$ may be obtained by using Eq. (15), but a method of determining $m$ is necessary. Thus when the slope of the bump is such that $m$ is 1:1, the total diffuse light collected in the spectrometer is about 1 in $10^6$ (for $\sigma = 200$ Å, $\lambda = 4200$ Å). If $m$ is 1:100, the diffuse scattered light contributes 1% to the total reflection. Judging from our electron micrograph studies of surfaces of anthracene, there are a number of steps on the crystal surface, so that the lower values of $m$ may be more realistic. Perhaps it may be possible to determine $m$ experimentally by observing the variation of $R(\omega)$ with $\Delta\theta$ at a given wavelength.

Coherent scattering caused by surface roughness and its consequences have been well investigated in metals[40] being associated with the roughness induced excitation of the surface plasmon[41] which in a perfect crystal is a nonradiative excitation. Evidence for the breakdown of its nonradiative character in a real metal has been observed recently.[42] To provide a basis for quantitatively estimating the extent that the surface affects $R(\omega)$ by coherent scattering of the photon beam, we use two approaches: a semiclassical theory developed by Fedders[43] for surface plasmons and a classical theory developed by Berreman[44] to calculate the effect of surface roughness in the vicinity of a resonance when retardation is neglected.

Fedder's theory for surface plasmons in metals is applied to the case of surface excitons in molecular crystals by equating the shift of the frequency of the surface exciton above the bulk resonance frequency $(\omega_s - \omega_0)$ to that of the surface plasmon $\omega_s$ realizing that the resonance frequency of transverse excitations in a metal is zero. A surface may be represented in terms of its Fourier components by

$$z + \sum_n a_n \sin(\mathbf{q}_n \cdot \rho + \alpha_n) = 0\,, \qquad (17)$$

where $z=0$ for a perfect surface, $a_n$ and $\alpha_n$ are amplitudes and phases, $\mathbf{q}_n$ a wave vector on the $xy$ plane and $\rho$ a position vector in the same plane. The rms surface roughness $\sigma$ is given by

$$\sigma = b\left|\sum_n (a_n \mathbf{q}_n)^2\right|^{1/2} . \tag{18}$$

Neglecting the effects of a nonzero imaginary part of $\epsilon(\omega)$, one may calculate $\Delta R$, the average decrease in reflectance, over the region of interest where

$$\Delta R = [1/(\omega_s - \omega_0)]\int_{\omega_0}^{\omega_s} [R_0(\omega) - R(\omega)]\, d\omega , \tag{19}$$

where $\omega_s$ is the surface mode resonant frequency, $\omega_0$ is the bulk mode resonant frequency, and $R_0(\omega)$ is the reflectance for a smooth surface. When the wave vector of incident light $\mathbf{k}$ $(\approx \omega_s/c) \ll \mathbf{q}_n$,

$$\Delta R = \sum_n 2\pi a_n^2 q_{nx}^2 \mathbf{k}/|\mathbf{q}_n| , \tag{20}$$

where $q_{nx}$ is the $x$ component of $\mathbf{q}_n$.

For one component of surface roughness (the sum must be truncated at some value of $n$ such that $|\mathbf{q}_n| < \pi/b$, where $b$ is a lattice parameter), then

$$\Delta R = 2\pi a_n^2 \mathbf{q}_n \mathbf{k} . \tag{21}$$

The surface roughness parameter $\sigma$ is $a_n \cdot \mathbf{q}_n \cdot b$ and $\Delta R$ may be calculated from values of $\mathbf{q}$, $b$, and $\mathbf{k}$. For roughness such that $\sigma$ is about 10 Å, with $b = 10$ Å, $\mathbf{k} = 2.5 \times 10^4$ cm$^{-1}$ and roughness wave vector $10^7$ cm$^{-1}$ structure with dips of 0.16 may occur in the normal incidence reflectance spectra. This of course is only a sample calculation to show that roughness induced excitation of surface excitons may have quite large effects on $R(\omega)$. The assumption involved in the calculation, viz., that the surface is of such periodicity as to be represented by a single Fourier component is necessarily a very crude one for a molecular crystal.

The above theory does not lend itself to illustrating the distorting effects on the line shape caused by surface roughness. From the viewpoint that surface roughness leads to displacement of the resonant frequencies from the bulk optic mode frequencies, Berreman's theory[44] is more suitable for calculating the effect of surface roughness on the spectrum in the vicinity of a resonance.

Let the surface be characterized by $N$ bumps or pits which are figures of revolution of average volume $V$. Then, following Berreman, the surface of the bump is divided into several collars each with a surface divergence $\sigma_{0j}(\omega) = \sigma_j(\omega)\cos\phi$ constant over the width of the collar, where $\cos\phi$ is measured from the direction of the applied field. Using the electrostatic boundary conditions, $\sigma_j$ is found by solving the simultaneous equations

$$\sum_j A_{ij}\sigma_j(\omega) + \frac{1}{2}\frac{1+\epsilon(\omega)}{1-\epsilon(\omega)}\sigma_i(\omega) = -\mathbf{E}_0 \cdot \mathbf{n}_i , \tag{22}$$

where $\mathbf{n}_i$ is the surface normal at $\phi = 0$ of collar $i$, $\epsilon(\omega)$ is that for the perfect crystal, $A_{ij}$ is the normal component of the electric field at $\phi = 0$ at the center of collar $i$ caused by a unit surface divergence (for $\phi \equiv 0$) of collar $j$, $\mathbf{E}_0$ is the electric field near the perfect surface equal to $2/[1+\sqrt{\epsilon(\omega)}]$.

Values of $A_{ij}$ were calculated for a bump defined by

$$\mathbf{r} = x\cos\alpha\hat{\mathbf{i}} + x\sin\alpha\hat{\mathbf{j}} + \tfrac{1}{2}a[1+\cos(\pi x/b)]\hat{\mathbf{k}} , \tag{23}$$

with

$$|\mathbf{r}| = 0 \quad \text{for} \quad -b > x > b ,$$

where $a$ is the height and $2b$ the width of the bump. To calculate $A_{ij}$, 12 collars were used with each collar divided into 10 rings. Values of $\sigma_j$ were solved from the simultaneous equations and the total horizontal dipole moment induced by the surface divergence was calculated:

$$P_H(\omega) = \frac{1}{4}\sum_j \sigma_j(\omega)\omega_j r_j^2 , \tag{24}$$

where $\omega_j$ is the width and $r_j$ the radius of collar $j$. The reflectance $R(\omega)$ of a crystal with a surface containing $N$ bumps or pits per unit area each of volume $V$ and of shape given by Eq. (23) is

$$R(\omega) = R_0(\omega)\left[1 + \frac{N}{\lambda} 16\pi^2 \mathrm{Im}\left(\frac{P_H(\omega)(\epsilon+1)}{\epsilon-1}\right)\right]$$

$$= R_0(\omega)[1 + (NV/\lambda)\vartheta(\omega)] , \tag{25}$$

where $\vartheta$, a form factor, is equal to

$$4\pi\,\mathrm{Im}\left(\frac{4\pi}{V}P_H(\omega)\frac{\epsilon+1}{\epsilon-1}\right) .$$

The form factor has its largest values when $\epsilon_r \approx -1$ and $\epsilon_i$ is small. Note that the condition $\epsilon_r \approx -1$ is the requirement for the excitation of surface modes. We interpret Berreman's theory as a classical calculation in the macroscopic dielectric approximation (without inclusion of retardation) of the effects of the surface roughness induced excitation of the nonradiative surface modes. Obviously, the theory is valid only in the long wave approximation $NV \ll \lambda$.

The effect of surface roughness on a crystal whose reflectivity is given by the model of Sec. II is shown in Fig. 7. Note that the spectrum of $\vartheta(\omega)$ has two peaks at $\epsilon \approx -1$ and $+1$. A decrease in $R(\omega)$ is always calculated ($\vartheta$ negative), being larger on the high energy side (in the region of negative $\epsilon_r$). Also note that $R(\omega)$ becomes more distorted with increasing surface roughness, as shown in Fig. 7(b). This distortion is a strong function of $\vartheta$, which in turn is dependent on the values of $\epsilon_i$ and $\epsilon_r$. At room temperature, we have measured the minimum value of $\epsilon_r$ to be 1.5 (at 25 567 cm$^{-1}$) at which $\epsilon_i = 2.8$. This gives a value for $\vartheta$ of 1.5, so that at $\lambda = 4000$ Å, with $NV$ approximated at about 50 Å (cf. the rms roughness of a sublimation flake, Sec. III. C. 1), the maximum percentage change in $R$ is 2%.

As the temperature decreases, $|\vartheta|$ increases and the band distortion for a crystal of given surface roughness can be quite marked. The measured reflection coefficient at low temperatures may be some 20% below the value of a perfect surfaced crystal in the region $\epsilon_r \approx -1$. To estimate the distortion in a reflection experiment upon a specific crystal, it would be useful to know the value of

$NV$ which might be obtained from surface holography. Alternatively, the value of $\sigma$, the rms roughness parameter discussed earlier, would provide an upper limit of $NV$. Also, since the distortion expected is a linear function of $NV$ for $NV \ll \lambda$ [see Eq. (25)], if two reflectance spectra were obtained for crystals of known $NV$ (or $\sigma$), an undistorted spectrum would be obtainable. Just how much distortion of $\epsilon(\omega)$ related to surface roughness occurs in a measurement on a real crystal is now known, but if $m$, the rms slope of the surface profile, was very small, then the long wave approximation $NV \ll \lambda$ in Berreman's method may not be adequate. It would be very useful if retardation were taken into account in this theory as this would provide more realistic results for large $NV$ values. As it stands, the theory does overemphasize the effect of distortions in that situation so that we would not anticipate such large effects as shown in Fig. 7 for large $NV$.

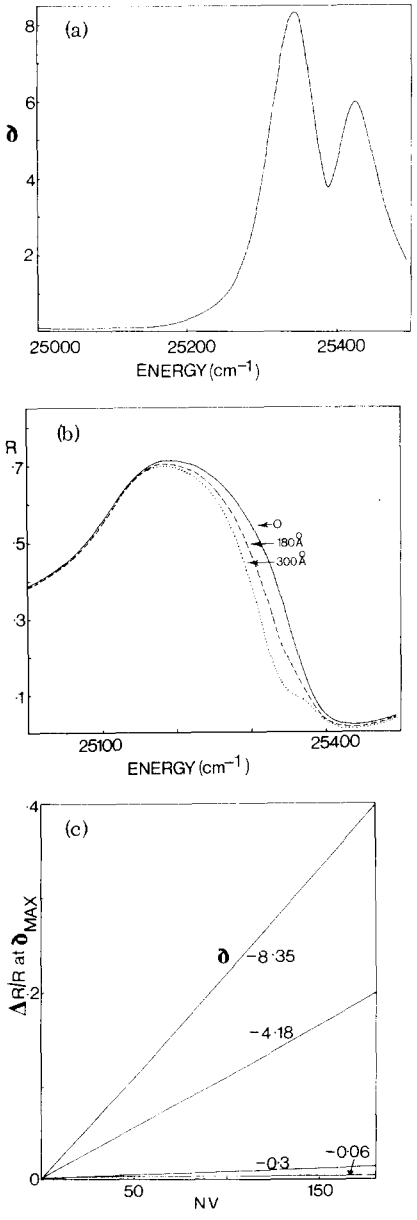


FIG. 7. Effect of surface roughness on an anthracene crystal whose reflectance was originally that of a semi-infinite perfect crystal. (a) Spectrum of the form factor $\partial(\omega) = 4\pi \operatorname{Im} | (4\pi/V) p_H(\omega) (\epsilon+1)/(\epsilon-1) |$; (b) $R(\omega)$ for different values of $NV$ the surface roughness parameter $R(\omega) = R_0(\omega) | 1 + (NV/\lambda) \partial(\omega) |$; (c) Variation in $R(\omega)$ $[\Delta R/R = (NV/\lambda) \partial(\epsilon_r, \epsilon_i)]$ for different values of $NV$ and $\partial$.

## 2. *Internal roughness: Impurities, defects, bulk inhomogeneities*

The effects of impurities, voids, dislocations, displaced molecules, etc. on the profile of $\epsilon(\omega)$ for a moderately strong optical transition is little known.

A possible approach to the problem of determining how impurity states will affect the spectral distribution $\epsilon(\omega)$ and hence $R(\omega)$ is by consideration of the interactions between the impurity states and the host crystal states using deep and shallow trap theory.[45–47] In particular, Hoshen and Jortner[47] have obtained the optical line shape of mixed crystals for reasonably high concentrations of a dopant and for weak optical transitions. For an intense transition and in a crystal with residual (and therefore low) impurity or defect concentration, as would be the case for the "pure" crystals used in reflection spectroscopy, we approach the problem by focusing attention on the alterations in the macroscopic dielectric field in the solid but neglecting the alterations in the short range interactions caused by introduction of defects, etc. This parallels our treatment of the surface modes and becomes a more reasonable approach as the intensity of the absorption increases.

For a transition with a moderate oscillator strength when $\epsilon_r$ for the bulk material is negative, molecules surrounding the defects may be set in resonance (similar to the effect of molecules on a surface resonating when $\epsilon = -1$). The situation is that of a trapped exciton in the region of a lattice defect for which extensive experimental evidence exists in molecular crystals probed by reflection and emission spectroscopy.[23] If the impurity molecule has a resonance energy such that the exciton is coupled to the vibronic states of the impurity molecule, the initial exciton state becomes broadened owing to the finite lifetime of the impurity vibronic state. The transition probability for such a process[48] is proportional to $(1-\epsilon)/(\epsilon+\frac{1}{2})$. For a weak transition $\epsilon$ is positive and nearly constant, but for a strong transition, $\epsilon$ may become negative and the term $(1-\epsilon_r)/(\epsilon_r+\frac{1}{2})$ resonates at $\epsilon_r = -\frac{1}{2}$.[49] This occurs within the exciton band, i.e., $\omega_0 < \omega < \omega_L$, and the presence of impurities (in general, inhomogeneities) will cause strong absorption within the exciton band when $\epsilon_r < 0$. The host crystal is, of course, strongly absorbing in this range, but distortion of its absorption profile may occur. The observation that $\epsilon_r$ becomes negative for a strong transition (provided that the damping due to third body interactions in a perfect crystal are not too large) may well be important in determining the exciton dynamics in such systems.

To obtain quantitative data on how this effect will perturb the model of $\epsilon(\omega)$ for a perfect infinite crystal, we approach the problem in two ways: (a) use of Galeener's theory[50] developed for studying the effects of voids on

the optical properties of semiconductors; (b) use of theories developed to understand the propagation of light through inhomogeneous media, [51] which may be applied[52] to the study of optical properties of imperfect crystals.

(*a*) *Distortion of* $R(\omega)$ *and* $\epsilon(\omega)$ *of a perfect host crystal by voids in the bulk.* Let $\eta$ be the percent volume of material occupied by inhomogeneities (voids) and $L$ be the depolarization factor[53] for the axis of the inhomogeneity parallel to the field $\mathbf{E}(r)$ due to a dipole at $r$, where $0 \leq L \leq 1$. Let the bulk crystal be isotropic with the inhomogeneities represented as ellipsoids of revolution (of dimensions less than the wavelength of light) with an axis parallel to the wave vector of light. In this case, the effective dielectric permittivity $\epsilon_e(\omega)$ is given for $\eta \ll 1$ by

$$\epsilon_e(\omega) = \epsilon(\omega)(1 + \tfrac{2}{3}\eta\pi_v)/(1 - \tfrac{1}{3}\eta\pi_v) \ . \tag{26}$$

where

$$\pi_v = \frac{1 - \epsilon(\omega)}{L + (1 - L)\epsilon(\omega)} \ . \tag{27}$$

The effective reflectance of the crystal is given by

$$R_e(\omega) = \left| [\epsilon_e^{1/2}(\omega) - 1]/[\epsilon_e^{1/2}(\omega) + 1] \right|^2 \ . \tag{28}$$

In Fig. 8 are shown the calculated errors in $R_e(\omega)$ and the imaginary part of $\epsilon_e(\omega)$ at the peak positions of the perfect crystal due to various percent volume of defects and for different values of $L$. Note that for errors in $\Delta R$ of less than 1%, the percent volume of defects in the crystal for all values of $L$ must be less than $10^{-3}$. In general, for molecular crystals, the average concentration of impurities, defects, voids, etc., would appear to be less than this.[6] However, in a strongly absorbing crystal system, the number of defects localized near the surface is in our opinion the meaningful value and in view of the photochemical reactivity of anthracene,[54] we do not know what this concentration or the distribution would be. In Fig. 9, we show how a 2% concentration of impurities, voids, etc., will provide an internal roughness to alter both $R(\omega)$ and $\epsilon_i(\omega)$ of the perfect crystal model. As $L$ increases, the resonant frequency shifts to higher energy and the maximum of $\epsilon_i(\omega)$ is increased. Considerable distortion is introduced in the low energy absorption edge. As $L$ decreases, e.g., near 0.9, a small resonance (from molecules near the inhomogeneity) appears in the spectrum of $\epsilon_i(\omega)$ where $\epsilon_r(\omega) = -1.22$) and is even more apparent in the reflectance spectrum due to its dispersive nature. Neglecting damping this resonance occurs in general when $\epsilon_r = -L/(1 - L)$. Hence, depending on the shape of the inhomogeneity, these resonances occur in the region from $\omega_0$ ($\epsilon_r = -\infty$, $L = 1$) to $\omega_L$ ($\epsilon = 0$, $L = 0$), with that for a sphere ($L = \frac{1}{3}$) occurring at $\epsilon = -\frac{1}{2}$. When damping is included, we expect that the resonance with $L \approx 1$ will be rapidly damped out ($\epsilon_i$ large near $\omega_0$). Note that the effect of inhomogeneities on the reflection spectrum is to reduce the reflectance on the low energy side. This is opposite to the effect on $R(\omega)$ produced by surface roughness discussed earlier (cf. Fig. 7).

(*b*) *The optical parameters in the region of impurity absorption in an inhomogeneous crystal.* Consider a perfect crystal of substance $A$ characterized by a dielec-

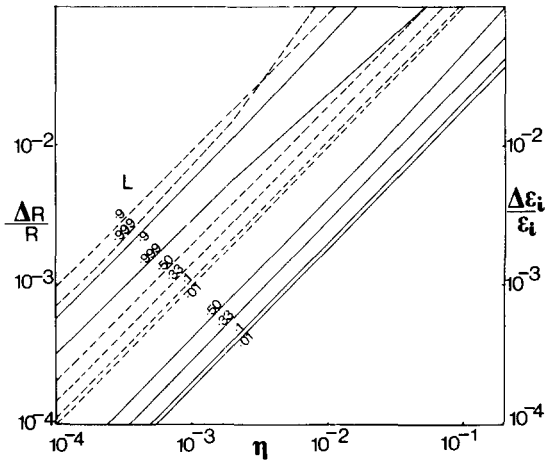


FIG. 8. Variation in the normal incidence reflectance $R(\omega)$ and the imaginary part of the dielectric permittivity $\epsilon_i(\omega)$ (calculated at the peak positions for the perfect crystal) for an anthracene crystal with various percent volume $\eta$ of internal roughness caused by defects, impurities, voids, etc., and with different values of the depolarization factor $L$. Solid line, $\Delta R/R$; dashed line, $\Delta\epsilon_i/\epsilon_i$.

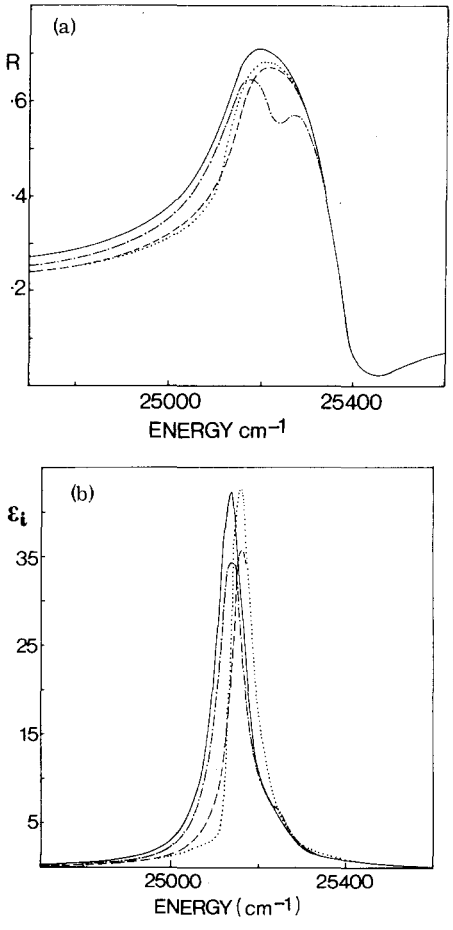


FIG. 9. The distortion of the normal incidence reflectance $R(\omega)$ (a) and the imaginary part of the dielectric permittivity $\epsilon_i(\omega)$ (b) from that of a perfect crystal when internal roughness caused by defects, impurities, voids, etc., of mole fraction 0.02 are added. Solid line, $\delta = 0$; dotted line, $L = 0.999$; dashed line, $L = 0.99$; dashed-dotted line, $L = 0.9$.

tric permittivity $\epsilon_A(\omega)$. Let the crystal be doped with mole fraction $N_B$ of substance $B$, which in a perfect crystal of $B$ is characterized by a dielectric permittivity $\epsilon_B(\omega)$. To determine the optical properties of the mixed crystal, it is necessary to calculate the dielectric permittivity $\epsilon_M(\omega)$ of the mixed crystal.

If the mixed crystal is optically homogeneous, then $\epsilon_M(\omega)$ is given by

$$\epsilon_M(\omega) = N_B\epsilon_B(\omega) + (1 - N_B)\epsilon_A(\omega) \tag{29}$$

and the reflectance

$$R_M(\omega) = \left| [\epsilon_M^{1/2}(\omega) - 1]/[\epsilon_M^{1/2}(\omega) + 1] \right|^2 . \tag{30}$$

The optical properties related to the impurity molecules are simply proportional to their concentration.

If the mixed crystal system is considered as inhomogeneous, then $\epsilon_M(\omega)$ is variable throughout the crystal bulk. The fluctuation $\delta(\omega)$ of the dielectric permittivity may be taken as $\delta(\omega) = |\epsilon_A(\omega) - \epsilon_B(\omega)|$, and the fluctuation of phase change upon reflection from the mixed crystal $\rho(\omega) = |\theta_A(\omega) - \theta_B(\omega)|$, where $\theta_A(\omega)$, $\theta_B(\omega)$ are the phase changes upon reflection from pure $A$ and pure $B$. This form for $\rho(\omega)$ will overemphasize effects in the limit of low concentration. The fluctuations in $\epsilon(\omega, \mathbf{r})$ from impurities and imperfections in an inhomogeneous media would be rapid. If the fluctuations in $\epsilon(\omega, \mathbf{r})$ are assumed stochastic and isotropic, with a fluctuation autocorrelation function of the (Markov) form

$$\langle \epsilon'(\omega, r)\epsilon'(\omega, 0)\rangle = \delta^2(\omega)\exp[-(8\pi)^{1/3}r/a_0] , \tag{31}$$

where $a_0$ is the fluctuation correlation length and $\epsilon'(\omega, r) = \epsilon(\omega, r) - \epsilon_M(\omega)$ then it is possible to calculate the effective reflectance of the impure crystal as follows.[51] If $n_M(\omega) = \epsilon_M(\omega)^{1/2} = n_M^r(\omega) + i\kappa_M^r(\omega)$, then an effective refractive index $n_e(\omega)$ and effective absorption index $\kappa_e(\omega)$ are given by

$$n_e(\omega) = n_M(\omega)n_x(\omega) , \tag{32}$$

$$\kappa_e(\omega) = \kappa_M(\omega)\,\frac{2n_x(\omega)^2 - 1}{n_x(\omega)} + \frac{\delta(\omega)^2 n_M(\omega)^4\omega^3 a_0^3}{24\pi n_x(\omega)c^3} , \tag{33}$$

where

$$n_x(\omega) = \left(1 + \frac{\pi^{-2/3}\delta^2(\omega)n_M^2(\omega)\omega^2 a_0^2}{6c^2}\right)^{1/2} , \tag{34}$$

provided $a_0 \ll \lambda/n_M(\omega)$ (small correlation length) and $n_M(\omega) \gg \frac{1}{2}\kappa_M(\omega)$ (small absorption). Obviously, $n_e(\omega) + i\kappa_e(\omega) \to n_M(\omega) + i\kappa_M(\omega)$ when $a_0 \to 0$ and/or $\delta(\omega) \to 0$.

The reflectance $R(\omega)$ may be defined as

$$R(\omega) = \left| \frac{n_e(\omega) - 1 + i\kappa_e(\omega)}{n_e(\omega) + 1 + i\kappa_e(\omega)} \right|^2 \tag{35}$$

and for the effect of diffuse scattering due to the phase fluctuations caused by the inhomogeneity of the crystal[52] (analogous to the diffuse scattering caused by rough surfaces),

$$R_D(\omega) = R(\omega)e^{-\rho(\omega)^2} . \tag{36}$$

To illustrate the effects of inhomogeneities we calculate $R(\omega)$, $R_D(\omega)$, and $R_M(\omega)$ for a crystal which has an impurity of mole fraction 0.02. The intention of this sample calculation is to see how the reflectance of a crystal with a moderately intense and broad resonance is affected by the presence in the crystal of impurities which themselves are weakly absorbing with narrower resonances. We assume that a Lorentzian line profile is a suitable model to describe $\epsilon(\omega)$ of both the host crystal and a crystal only composed of molecules of the impurities. The parameters used in Eq. (1) to give $\epsilon(\omega)$ for the host crystal are $\epsilon_0 = 6.4$, $\gamma = 75$, $f = 0.01$, and $\omega_0 = 25127$ cm$^{-1}$. For the crystal composed of only impure molecules, the parameters are $\epsilon_0 = 6.4$, $\gamma = 15$ cm$^{-1}$, $f = 0.001$, and $\omega_0 = 24100$ cm$^{-1}$ to obtain data related to a deep lying trap and $\omega_0 = 25100$ cm$^{-1}$ to obtain data related to a shallow lying trap.

In the calculations, no account is taken of resonance effects such as intensity stealing from the host exciton band arising from changes in the short range forces. Especially when the trap is shallow lying, allowance for "giant" oscillator strengths[55] could enhance the effects to be described. In Fig. 10 are plotted the reflectance data in the cases where the impurity forms a deep trap [Fig. 10(a)] of depth 1027 cm$^{-1}$ or a shallow trap [Fig. 10(b)] of depth 27 cm$^{-1}$. Two values of $a_0$ were used for the calculations, viz., 10 and 100 Å. We believe that the small value of the correlation length corresponds to what would be expected in the amalgamation limit in calculations using the coherent potential approximation.[46,47] The large value of $a_0$ would correspond to the persistence limit.

For the deep trap case, note: (i) When $a_0 = 10$ Å (a molecular spacing), if optical phase fluctuations are neglected then the spectrum $R_M(\omega)$ is indistinguishable from $R(\omega)$. When allowance is made for such fluctuations, then a reflectance dip in $R_M(\omega)$ will occur in the frequency region where the longitudinal mode would propagate in the crystal of impure molecules. The optical phase change is a maximum at this frequency and its position is independent of $a_0$ and concentration of impurity in the mixed crystal. (ii) When $a_0 = 100$ Å (corresponding to some aggregation of defects and impurities) it is seen that narrow structures in $R(\omega)$ and $R_D(\omega)$ is observed. These structures appear at the frequencies of the transverse and longitudinal optic modes expected in a crystal of impure molecules $A$. When optical phase fluctuations are neglected, the low energy structure is only at the frequency of the transverse optic mode. The intensity of the dip in $R(\omega)$ is dependent upon the value of $\epsilon_0$ which should be less than 6.4 in this region. A lowered value of $\epsilon_0$ would enhance the effect shown.

For the shallow trap case, note: (i) When $a_0 = 10$ Å, structure in $R(\omega)$ is observed near the resonance frequency of the impurity, even when phase fluctuations are neglected. When they are considered, it is seen that they are enhanced over the deep trap case and a very prominent reflectance dip is observed at $\omega_L$ of a crystal composed of impure molecules. (ii) When $a_0 = 100$ Å, $R(\omega)$ shows reflectance dips as observed in the deep trap case, but also exhibits an interesting redistribution of intensity. The reflectance of the pure crystal is smoothly increasing to a peak at 25190 cm$^{-1}$. When impurities are embedded in the crystal, $R(\omega)$ is greater than the re-

flectance from either the pure host crystal or a crystal of impurity molecules in some regions of $\omega$.

We would suggest for molecular crystals that large values of $a_0$ are probably more appropriate when the effects of defects, etc., are considered, as these would be concentrated in regions rather than uniformly dispersed throughout the solid. In Fig. 10, there is a striking demonstration of how the $R(\omega)$ of an impure or defective crystal will exhibit pronounced narrow reflectance dips even though only a small mole fraction of impurities are present. It is worth emphasizing here that many methods of gauging impurity or defect concentration do provide an average value of such defects and not the distribution within the crystal. The optical reflection is very sensitive to the distribution as may be seen from the following. If a layer of a strongly absorbing impurity were lying in a plane parallel to, or on, the surface of an otherwise perfect crystal of semi-infinite size, the mole concentration of impurity would be negligible, but $R(\omega)$ would be strongly affected.

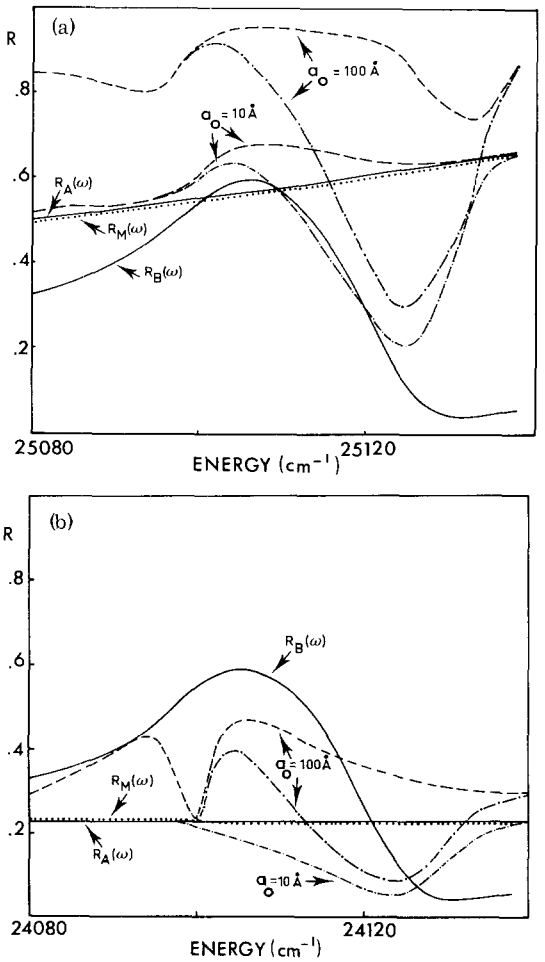


FIG. 10. The distortions in the normal incidence reflectance $R(\omega)$ caused by inhomogeneities of mole fraction 0.02 in an anthracene crystal when the inhomogeneity acts as a deep trap (a) and as a shallow trap (b). The resonance frequency of the trap is 24 100 cm$^{-1}$ (a) and 25 100 cm$^{-1}$ (b) and a crystal of the impurity molecules is assumed to have an $\epsilon(\omega)$ given by a Lorentzian line dielectric function model with $\epsilon_0 = 6.4$, $\gamma = 15$ cm$^{-1}$, $f = 0.001$. The pure anthracene crystal also has an $\epsilon(\omega)$ given by the same model with $\epsilon_0 = 6.4$, $\gamma = 75$ cm$^{-1}$, $f = 0.01$, and $\omega_0 = 25\,127$ cm$^{-1}$. Solid line, $R_A(\omega)$—the normal incidence reflectance of a pure anthracene crystal; dotted line, $R_M(\omega)$—the normal incidence reflectance of the mixed crystal considered optically homogeneous [see Eq. (30) in text]; solid line, $R_B(\omega)$—the normal incidence reflectance of a crystal composed of the impurity molecules only; dashed line, $R(\omega)$—the normal incidence reflectance of the mixed crystal considered optically inhomogeneous but neglecting phase fluctuations. Correlation length 10 Å [$\equiv R_M(\omega)$ in Fig. 10(a)] and 100 Å; dashed-dotted line, $R_D(\omega)$—the normal incidence reflectance of the mixed crystal considered optically inhomogeneous and allowing for phase fluctuations caused by inhomogeneity of the crystal. Correlation length 10 Å and 100 Å.

The reflectance spectrum of an anthracene crystal has been shown to exhibit a number of narrow reflectance dips both within[23,24] and to lower energy of[23] the main resonance region. In the earlier paper[23] the lower energy reflectance dips were argued to be evidence for the existence of impurities and defects in the crystal. At that stage, we could not decide whether we were observing an antiresonance behavior or an anomalous dispersion in an energy region close to that of the discrete impurity resonance. The latter explanation was suggested to be the correct one. The above calculations support that earlier interpretation of the data. They also illustrate very well an earlier comment[2] that an assignment of resolved reflectivity peaks in the region of the main absorption bands to phonon modes[24] is open to question in view of the effect which impurities may have on $R(\omega)$.

## V. SUMMARY AND CONCLUSIONS

An objective of this paper has been to provide methods for answering the question: "To what extent does the use in experiments of a finite imperfect crystal rather than an infinite perfect crystal invalidate an approach to understanding the exciton's dynamics through interpretation of $\epsilon(\mathbf{k}, \omega)$?" The methods developed relate to any crystal. In Table V are summarized the conditions, neglecting damping for excitation of quasiparticles, that produce the majority distortion in $\epsilon(\mathbf{k}, \omega)$ when the photon–crystal eigenmodes are strongly coupled. When damping is considered, the dielectric condition of Table V serves as the limiting situation.

The methods are illustrated by considering a molecular crystal, anthracene, which serves as a good test situation because of the amount of experimental and theoretical data available for the $b$ polarized 4000 Å crystal absorption system. Using a model of $\epsilon(\omega)$ which might reasonably correspond to that absorption system at low temperature, if crystal and molecular anisotropies are negligible, a number of conclusions are reached.

### 1. *For a perfect semi-infinite crystal*

(i) Spatial dispersion will have little effect upon $\epsilon(\omega)$ determined by a normal incidence experiment, unless through the dispersion of the damping parameters.

(ii) One of the modes is mechanical and localized near the surface.

(iii) When the damping parameters for the pole and zero are different, asymmetry is induced in $\epsilon_i(\omega)$, be-

TABLE V. Conditions under which quasiparticles are excited in finite imperfect crystals.

| Quasiparticle | Requirement for excitation | Dielectric condition neglecting damping |
|---|---|---|
| Transverse exciton | Any crystal | $\epsilon_r = \pm\infty$ |
| Longitudinal exciton | Semi-infinite crystal<br>Oblique incidence light<br>$P$ polarization | $\epsilon_r = 0$ |
| Surface exciton | Imperfect surface on semi-infinite crystal | $\epsilon_r = -1$ |
| Exciton at a defect | Imperfect crystal | $\epsilon_r = -(L/1-L)$ ($L$ is depolarization factor: $0 \le L \le 1$),<br>$\epsilon_r = 0$, $L = 0$, slab or longitudinal cylinder $\perp \mathbf{k}$<br>$\epsilon_r = -\frac{1}{2}$, $L = \frac{1}{3}$, sphere<br>$\epsilon_r = -1$, $L = \frac{1}{2}$, transverse cylinder<br>$\epsilon_r = -\infty$, $L = 1$, slab $\parallel \mathbf{k}$ |
| Radiative exciton | Finite crystal | $\epsilon_r = i\frac{\beta}{\alpha}\left[\frac{e^{-i\beta a} \pm e^{i\beta a}}{e^{-i\beta a} \mp e^{i\beta a}}\right]$ $P$ pol.<br>$1 = i\frac{\beta}{\alpha}\left[\frac{e^{-i\beta a} \pm e^{i\beta a}}{e^{-i\beta a} \mp e^{i\beta a}}\right]$ $S$ pol.<br>where $\beta = [\epsilon_r(\omega^2/c^2) - k_x^2]^{1/2}$<br>$\alpha = [k_x^2 - \omega^2/c^2]^{1/2}$,<br>$2a$ = thickness |

coming greater as $\Gamma_z$ increases, so that the resonance frequency $\omega_0$ and the maximum value of $\epsilon_i(\omega)$ become separated. The positions of the maximum of the reflectance $R(\omega)$ is a very sensitive function of the asymmetry.

(iv) Frequency dependent damping parameters $\Gamma_p(\omega)$ and $\Gamma_z(\omega)$ are needed to describe adequately $\epsilon(\omega)$ for this system.

(v) When a non-normal angle of incidence is used as an approximation to normal incidence light, significant errors in $R(\omega)$ may occur. The relative distortion in $\kappa(\omega)$ is less than that in the other optical parameters.

(vi) We suggest that oblique angle spectroscopy can provide a useful method to probe exciton dispersion around $\mathbf{k} = 0$.

(vii) At oblique angles of incidence, longitudinal modes will propagate when $\epsilon$ has a minimum absolute value. There may be evidence from previous experiments for the frequency position where these longitudinal modes propagate. In a sample calculation, we show the structure in $R(\omega)$ expected when a longitudinal mode exists and show that the unambiguous interpretation of structure in $R(\omega)$ is not without difficulties. A measure of the angular dependence of $R(\omega)$ should help resolve the problems of interpretation.

### 2. *For a finite perfect crystal*

(i) Surface modes should be excited in the crystal when retardation is neglected.

(ii) When retardation is accounted for, there are both radiative modes, which interact with light in a normal optical experiment, and nonradiative modes, which interact with light as the crystal becomes less perfect, so that surface roughness may induce the excitation of surface exciton modes.

(iii) For a crystal of thickness greater than 1 $\mu$, $R(\omega)$ for normal incidence is sensibly independent of thickness, i.e., the effects of radiative broadening of the excited polariton state are negligible so that $R(\omega)$ is determined primarily by third body interactions.

(iv) For crystals of thickness less than 0.1 $\mu$, distortions appear in $R(\omega)$ and this suggests that care should be taken in interpreting thin film absorption or reflectance data.

### 3. *For a real semi-infinite crystal: Real surface but perfect bulk*

(i) Surface roughness reduces the reflectance $R(\omega)$ by incoherent and coherent scattering.

(ii) A knowledge of $\sigma$, the rms surface roughness, enables some correction to be made for incoherent scattering, provided there is negligible acceptance of the diffuse light by the detection system. When this latter is significant, it is further necessary to have some knowledge of the shape of the bumps giving rise to diffuse scattering so that the rms slope of the surface profile may be used to determine the amount of diffuse light measured in the spectrometer. We suggest ways of measuring both $\sigma$ and $m$.

(iii) The consequences of coherent scattering are in-

vestigated by two means: use of a semiclassical theory developed for surface plasmons[43] and use of a classical theory.[44] The semiclassical calculations illustrate how roughness induced excitation of surface excitons may have large effects on $R(\omega)$, but the application of the method is limited in that the assumption invoked in our calculations is that the surface is of such periodicity as to be represented by a single Fourier component. The classical theory is used in a model calculation to show how surface roughness will distort $R(\omega)$. We show that at room temperature, the maximum percentage change in $R$ is about 2% calculated from use of our experimental values of $\epsilon_r$, $\epsilon_i$, and $\sigma$, the rms surface roughness. As the crystal temperature is decreased, $\epsilon_r$ and $\epsilon_i$ alter appreciably and quite marked distortions in $R(\omega)$ appear. It would be useful if the theory on which the calculations were based was extended to include retardation effects. As it stands, it overemphasizes the distortions as the surface roughness increases.

Clearly, it is necessary that some evaluation of the quality of the surface of a molecular crystal be achieved, for this will decide the adequacy of the long wave approximation in the classical theory and may enable development of a suitable analytic expression for the surface.

### 4. *Real semi-infinite crystal: Internal roughness*

(i) We illustrate how $R(\omega)$ and $\epsilon(\omega)$ of the perfect crystal are affected by voids in the real crystal bulk using Galeener's theory[50] to calculate the errors in $R(\omega)$ and $\epsilon_i(\omega)$ as a function of the concentration of defects of various shapes. In a sample calculation we show how structure in $R(\omega)$ may be caused by such defects and how these defects reduce the reflectance on the low energy side, an effect opposite to that resulting from surface roughness.

(ii) We show the effect of both a deep and a shallow trap upon $R(\omega)$ by determining the optical properties of a mixed crystal. If the crystal is optically homogeneous, the optical properties related to the impurity molecules are simply proportional to their concentration. When the system is considered inhomogeneous, with fluctuations in $\epsilon(\omega, \mathbf{r})$ assumed stochastic and isotropic, then the optical properties of a crystal with mole fraction 0.02 of a weakly absorbing impurity molecule will be dependent on the correlation length $a_0$ of the fluctuations. We consider the limits $a_0 = 10$ Å, a molecular spacing corresponding to the amalgamation of the impurity molecules and the host molecule in the crystal lattice, and $a_0 = 100$ Å, corresponding to an aggregation of defects and impurities (persistence limit). We expect that the latter is more likely to be the situation occurring in a real molecular crystal. In sample calculations, we illustrate how structure appears in $R(\omega)$. When optical phase fluctuations are taken into account, prominent reflectance dips occur as $a_0$ increases at the frequencies of the transverse and longitudinal optic modes expected in a crystal composed only of the impurity molecules. In the case of a shallow trap, an interesting redistribution of intensity in $R(\omega)$ occurs.

What then are the implications of these findings for using reflection spectroscopy to provide $\epsilon(\omega)$ data as a probe of exciton dynamics in cases when the crystal eigenmodes and the photon are strongly coupled? In general, the more strongly coupled the system, the more severe the problems. At present the indications are that room temperature measurements with carefully collimated normal incidence light will give reflectance data $R(\omega)$ for anthracene crystals of suitable thickness, providing data which are useful for probing the exciton dynamics.[3] However, as the temperature is decreased and $\epsilon_i$ and $\epsilon_r$ alter, the extent of contributions to the line shape of $R(\omega)$ from surface and internal roughness will become more important and the data on exciton dynamics obtained on a real crystal become less related to the expected dynamics in a perfect crystal. To what extent the defects and impurities will cause problems of interpretation is as yet unknown. At present, it seems to us that the contribution to the line shape of $R(\omega)$ from surface roughness is probably the major problem and methods of estimating its extent have been discussed in the text. Further help with the problems would be achieved by using a less strongly absorbing crystal face and two photon methods to probe exciton–phonon interactions in the bulk.

*Note added in proof*: Several of the experiments suggested in this paper have been completed. See G. C. Morris and M. G. Sceats, Chem. Phys. **1**, 259 (1973); *ibid.* **1**, 376 (1973) and (to be published); Mol. Cryst. Liq. Cryst. (to be published).

## ACKNOWLEDGMENTS

This work was supported by the Australian Research Grants Committee and by the Commonwealth Scientific and Industrial Research Organization (a scholarship to M.G.S.).

[1](a) P. Avakian, V. Ern, R. E. Merrifield, and A. Suna, Phys. Rev. **165**, 974 (1968); (b) P. Avakian and R. E. Merrifield, Mol. Cryst. **5**, 37 (1969); (c) G. A. George and G. C. Morris, Mol. Cryst. Liq. Cryst. **10**, 115 (1970); (d) A. H. Francis and C. B. Harris, Chem. Phys. Letts. **9**, 181 (1971); **9**, 188 (1971); J. Chem. Phys. **55**, 3595 (1971).
[2]G. C. Morris, S. A. Rice, M. G. Sceats, and A. E. Martin, J. Chem. Phys. **55**, 5610 (1971).
[3]G. C. Morris and M. G. Sceats, Chem. Phys. 1, 120 (1973).
[4](a) A. S. Davydov, Phys. Status Solidi **20**, 143 (1967); (b) A. S. Davydov and E. N. Myasnikov, Dokl. Akad. Nauk SSR **171**, 1069 (1966) [Sov. Phys. Dokl. **11**, 1073 (1967)]; Phys. Status Solidi **20**, 153 (1967); (c) B. M. Nitsovich, Fiz. Tverd. Tela **9**, 2230 (1967) [Sov. Phys.-Solid State **9**, 1749 (1968)]; (d) S. Fischer and S. A. Rice, J. Chem. Phys. **52**, 2089 (1970); (e) M. K. Grover and R. Silbey, J. Chem. Phys. **52**, 2099 (1970).
[5]M. G. Sceats and G. C. Morris, Phys. Status Solidi A **14**, 643 (1972).
[6]See S. A. Rice, G. C. Morris, and W. L. Greer, J. Chem. Phys. **52**, 4279 (1970), and references therein.
[7]G. D. Mahan and G. Obermair, Phys. Rev. **183**, 834 (1969).
[8]M. R. Philpott, J. Chem. Phys. **56**, 996 (1972).
[9]We had earlier noted (Ref. 2) that theories of exciton–phonon scattering based on short range interactions (i.e., nearest neighbour only) are good approximations for an anthracene

crystal even when long range interactions are large. The calculations of Philpott (in Ref. 8) provide an understanding for this.

[10](a) C. W. Deutsche and C. A. Mead, Phys. Rev. **158,** A63 (1965); (b) T. Skettrup and A. Balsev, Phys. Rev. B **3,** 1457 (1971).

[11](a) Y. Osaka, Y. Imai and Y. Takeuti, J. Phys. Soc. Jap. **24,** 236 (1968); (b) S. I. Pekar, Zh. Eksp. Teor. Fiz. **33,** 1022 (1957) [Sov. Phys.-JETP **6,** 785 (1958)].

[12]J. J. Hopfield and D. G. Thomas, Phys. Rev. **132,** 563 (1963).

[13]J. J. Hopfield, J. Phys. Soc. Jap. Suppl. **17,** (1966).

[14]D. W. Berreman and F. C. Unterwald, Phys. Rev. **174,** 791 (1968).

[15](a) A. S. Davydov and E. F. Sheka, Phys. Status Solidi **11,** 877 (1965); (b) M. R. Philpott, J. Chem. Phys. **54,** 111 (1971).

[16]In calculating static exciton properties such as Davydov splitting, damping is not taken into account and the effect described here should be noted when comparing experimental results with theoretical calculations.

[17]In an earlier paper (Ref. 2) we noted a general lack of smoothness in our $\kappa(\omega)$ curves derived by use of a general dispersion relationship. We now understand this as arising from noncausal regions of $\epsilon(\omega)$ at frequencies below 25 100 $cm^{-1}$ indicative of the need to choose frequency dependent damping parameters.

[18]R. H. W. Graves, J. Opt. Soc. Am. **59,** 1225 (1969).

[19]L. B. Clark and M. R. Philpott, J. Chem. Phys. **53,** 3790 (1970).

[20]D. W. Berreman, Phys. Rev. **130,** 2193 (1963).

[21]M. M. Hargreaves, J. Phys. C **4,** 174 (1971).

[22]J. B. Bates and M. H. Brooker, J. Phys. Chem. Solids **32,** 2403 (1971).

[23]G. C. Morris, S. A. Rice and A. E. Martin, J. Chem. Phys. **52,** 5149 (1970).

[24](a) S. V. Marisova, Opt. Spectrosc. **22,** 310 (1965); Ukr. Fiz. Zh. **12,** 521 (1967); (b) M. S. Brodin, S. V. Marisova, and S. A. Shturkhetskaya, Urk. Phys. J. **13,** 249 (1968).

[25]Experiments carried out while this paper was in press suggest that the prominent dip at 25 290 $cm^{-1}$ is a resonance related to crystal strain effects. See G. C. Morris and M. G. Sceats, Chem. Phys. **1,** 376 (1973).

[26]W. C. Tait and R. L. Weiher, Phys. Rev. **166,** 769 (1968).

[27]R. Silbey, J. Chem. Phys. **46,** 4029 (1968).

[28]V. M. Agranovich, Zh. Eksp. Teor. Fiz. **37,** 430 (1959) [Sov. Phys.-JETP **10,** 307 (1960)].

[29]J. J. Hopfield, Phys. Rev. **112,** 1555 (1958).

[30]D. P. Craig and L. A. Dissado, J. Chem. Phys. **48,** 516 (1968).

[31]R. Fuchs and K. L. Kliewer, Phys. Rev. **140,** A2076 (1965).

[32]W. E. Jones and R. Fuchs, Phys. Rev. B **4,** 3581 (1971).

[33]V. I. Sugakov, Fiz. Tverd. Tela **5,** 2207 (1963) [Sov. Phys.-Solid State **5,** 1607 (1964)]; **5,** 2682 (1963) [**5,** 1959 (1964)].

[34]S. A. Rice and J. Jortner, *"Physics and Chemistry of the Organic Solid State*, edited by D. Fox *et al.* (Interscience, New York, 1967), Vol. III, Chap. 4.

[35]K. L. Kliewer and R. Fuchs, Phys. Rev. **144,** 495 (1966); **150,** 573 (1966).

[36]D. P. Craig and L. A. Dissado, Proc. Roy. Soc. A **332,** 419 (1973); **325,** 1 (1971).

[37]A similar method has been used to detect nonradiative surface plasmons in metals: A. Otto, Z. Phys. **216,** 398 (1968); **219,** 227 (1969).

[38]H. Davies, Proc. Inst. Elect. Eng. **101,** 209 (1954).

[39]H. E. Bennett and J. O. Porteus, J. Opt. Soc. Am. **51,** 123 (1961).

[40](a) A. Dande, A. Savary, and S. Robin, J. Opt. Soc. Am. **62,** 1 (1972); (b) S. N. Jasperson and S. E. Schnattery, Phys. Rev. **188,** 759 (1969); (c) E. A. Stern, Phys. Rev. Lett. **19,** 1321 (1967); (d) P. A. Fedders, Phys. Rev. **165,** 580 (1968); (e) R. H. Ritchie and R. E. Wilems, *ibid.* **178,** 372 (1969); **184,** 254 (1969); (f) J. Crowell and R. H. Ritchie, J. Opt. Soc. Am. **60,** 794 (1970); (g) J. M. Elsom and R. H. Ritchie, Phys. Rev. B **4,** 4129 (1971).

[41]N. Marschall, B. Fischer and H. J. Quetsser, Phys. Rev. **27,** 95 (1971).

[42]A. J. Braundkeier, Jr., M. W. Williams, E. T. Arakawa, and R. H. Ritchie, Phys. Rev. B **5,** 2754 (1972).

[43]P. A. Fedders, Phys. Rev. **165,** 580 (1968).

[44]D. W. Berreman, Phys. Rev. B **1,** 381 (1970); Phys. Rev. **163,** 855 (1967); J. Opt. Soc. Am. **60,** 499 (1970).

[45](a) D. P. Craig and M. R. Philpott, Proc. R. Soc. Lond. **A293,** 213 (1966); **A290,** 583 (1966); (b) E. I. Rashba, Opt. Spektrosk. **2,** 568 (1957); (c) V. L. Broude and E. I. Rashba, Fiz. Tverd. Tela **3,** 1941 (1961) [Sov. Phys.-Solid State **3,** 1415 (1962)]; (d) I. S. Osakdo, *ibid.* **11,** xxx (1969) [**11,** 347 (1969)]; (e) R. G. Body and I. G. Ross, Aust. J. Chem. **19,** 1 (1966).

[46]D. Fox, J. Chem. Phys. **54,** 2132 (1971).

[47]J. Hoshen and J. Jortner, J. Chem. Phys. **56,** 933 (1972); **56,** 5550 (1972).

[48]P. P. Schmidt, J. Chem. Phys. **52,** 1250 (1970).

[49]This is because the field due to a dipole at $\mathbf{r}$ in a medium of dielectric permittivity $\epsilon_r$ is $E(r) = 3/2(\epsilon_r + \frac{1}{2}) \cdot \mathbf{E}_m(r)$, where $\mathbf{E}_m(r)$ is the field due to a dipole in vacuum.

[50]F. L. Galeener, Phys. Rev. Lett. **27,** 421 (1971).

[51](a) R. C. Bourret, Can. J. Phys. **40,** 782 (1961); Nuovo Cimento **26,** 1 (1962); (b) V. I. Tatarski and M. E. Gertsenshtein, Zh. Eksp. Teor. Fiz. **44,** 676 (1963) [Sov. Phys.-JETP **17,** 458 (1963)]; (c) V. I. Tatarski, *ibid.* **46,** 1399 (1964) [**19,** 946 (1964)].

[52]I. Filinski, Phys. Status Solidi B **49,** 577 (1972).

[53]C. Kittell, *Introduction to Solid State Physics*, 3rd edition (Wiley, New York, 1967), p. 367.

[54](a) D. P. Craig and P. Sarti-Fantoni, Chem. Commun. **1966,** 742. (b) A. P. Rood, D. Emerson, and H. J. Milledge, Proc. R. Soc. **A324,** 37 (1971); (c) J. O. Williams and J. M. Thomas, Mol. Cryst. Liq. Cryst. **16,** 371 (1972).

[55]E. I. Rashba and G. E. Gurgenishvile, Fiz. Tverd. Tela **4,** 1029 (1962) [Sov. Phys.-Solid State **4,** 759 (1962)].